Proton Conducting Polymer Membranes: Synthesis & Characterization of Novel Sulfonated Polyimides

by

Olivier Savard
B.Sc. Université Laval 2002

THESIS SUBMITTED IN PARTIAL FULFILLMENT OF
THE REQUIREMENTS FOR THE DEGREE OF

MASTER OF SCIENCE

In the
Department
of
Chemistry

SIMON FRASER UNIVERSITY

Spring 2007

APPROVAL

Name: **Olivier Savard**

Degree: **Master of Science**

Title of Thesis: **Proton Conducting Polymer Membranes: Synthesis & Characterization of Novel Sulfonated Polyimides**

Examining Committee:

Chair: **Dr. Michael Eikerling**
Chair
Assistant Professor, Department of Chemistry

Dr. Steven Holdcroft
Senior Supervisor
Professor, Department of Chemistry

Dr. Ross Hill
Supervisor
Professor, Department of Chemistry

Dr. Hogan Yu
Supervisor
Professor, Department of Chemistry

Dr. Vance Williams
internal Examiner
Assistant Professor, Department of Chemistry

Date Approved: December 5th 2006

ABSTRACT

A new synthetic route to prepare the sulfonated monomer ((2,2'-bis(4-sulfobenzyloxy)benzidine), was developed. This and related compounds were characterized by ^{1}H and ^{13}C NMR, FTIR and EA. This new synthetic route provides access to a variety of new sulfonated monomers and polymers, which in turn facilitates studies of structure-property relationships of proton conducting membranes.

A series of novel membranes were prepared from the sulfonated polymer. This series of novel sulfonated polyimide membranes possesses higher hydrolytic stability than those prepared from polyimides in which the sulfonate groups are attached directly to the polyimide main chain, yet their proton conductivity is similar. The polymers were also characterized by nuclear magnetic resonance, differential scanning calorimetry, thermogravimetric analysis and in a fuel cell.

DEDICATION

À tous ceux et celles qui m'ont supporté durant cette étape de ma vie, qui a été à la fois enrichissante et éprouvante. Un merci tout spécial à ma famille, qui m'a donné force, encouragements et support pour me permettre de terminer en beauté! Je vous aime.

À mes ami(e)s du Québec qui, même à une si grande distance, ont su me redonner le sourire même dans les moments les plus difficiles.

À tous mes ami(e)s de Vancouver qui ont été à mes côtés au long de ma maîtrise. Une chance que je vous ai!

To my incredible lab mates. You are the best! Also, *un sincère merci* to my friends and teammates. I had so much fun with you!

Thank you to everyone else who helped me over the course of my degree. You are too many to name you all…

Et… À MOI!!! ☺

ACKNOWLEDGEMENTS

I would like to thank Dr. Steve Holdcroft for giving me the privilege of working under his supervision.

I would like to thank the members of my advisory committee, Dr. Ross Hill, Dr. Hogan Yu and Dr. Vance Williams.

I would like to thank Makoto Adachi for his help with the fuel cell test station, Marianne Rogers for performing DSC and TGA, Dr. Zhong Xie for making the MEAs, Jean-Claude Brodovitch for his help with the viscosity measurements and Dr. Miki Yang for performing the elemental analysis.

Many, many, many thanks to Dr. Tim Peckham for proof reading my masters thesis and to Dr. Yunsong Yang for his guidance and assistance.

Thank you to my lab mates for their support and encouragements.

TABLE OF CONTENTS

LIST OF FIGURES

LIST OF TABLES

LIST OF ABBREVIATIONS

2,2'-BSBB: 2,2'-bis(4-sulfobenzyloxy)benzidine
[ ]: Concentration
η_{red}: Reduced Viscosity
η_{inh}: Inherent Viscosity
η_{sp}: Specific Viscosity
η_r: Relative Viscosity
η: Viscosity
λ: Number of water molecules per sulfonic acid group
ρ: Partial pressure for the solution
ρ_0: Partial pressure for pure solvent
σ: Proton Conductivity
μSASX: micro Small-Angle X-ray Scattering
a-sPI: Angled Sulfonated Polyimide
AFC: Alkaline Fuel Cell
CCM: Catalyst Coated Membrane
CdI: Double Layer Capacitance
dL: deciliter
DMF: Dimethylformamide
DMSO: Dimethylsulfoxide
DSC: Differential Scanning Calorimetry
FTIR: Fourier Transform Infrared
g: gram
GDM: Gas Diffusion Media
HPM: Hot Pressed Membrane
IEC: Ion Exchange Capacity
l: length
l-sPI: linear Sulfonated Polyimide
MCFC: Molten Carbonate Fuel Cell
MEA: Membrane Electrode Assembly
MPL: Micro Porous Layer
NMR: Nuclear Magnetic Resonance
OCV: Open Circuit Voltage
N,N'-BDPMAP: N,N'-bis(diphenylmethylene)-o-aminophenol
PAEK: poly (aryl ether ketone)
PAFC: Phosphoric Acid Fuel Cell
PBI: poly(2,2'-(m-phenylene)-5,5'-dibenzidineimidazole
PEM: Proton Exchange Membrane
PEMFC: Proton Exchange Membrane Fuel Cell
PI: Polyimide
PSu: Polysulfone

RH: Relative Humidity
Rm: Membrane Resistance
Rs: Solution Resistance
s: second
SASX: Small Angle Scattering X-rays
SEM: Scanning Electron Microscopy
SOFC: Solid Oxide Fuel Cell
SPEEK: Sulfonated Poly (Ether Ether Ketone)
sPI: sulfonated Polyimide
t: thickness
TEM: Transmission Electron Microscopy
Tg: Glass Transition
TGA: Thermogravimetric Analysis
Tm: Melting Temperature
VU: Volume Uptake
w: width
WU: Water Uptake

LIST OF CHEMICALS

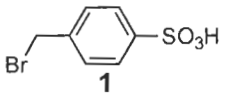

1

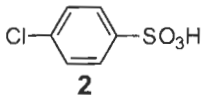

2

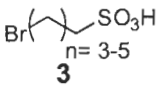

3

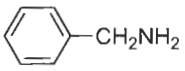

4

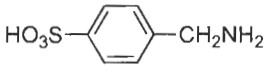

5

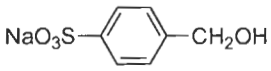

6

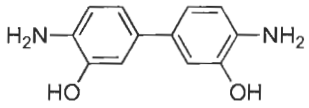

7

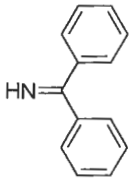

8

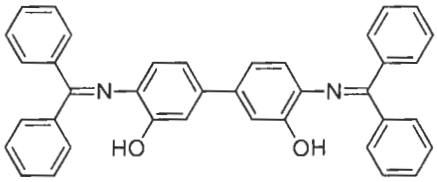

9

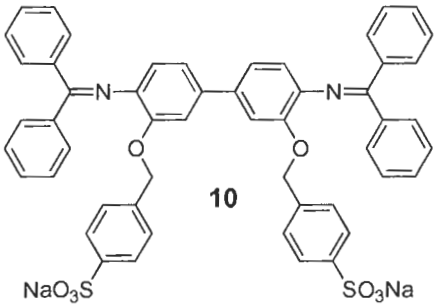

10

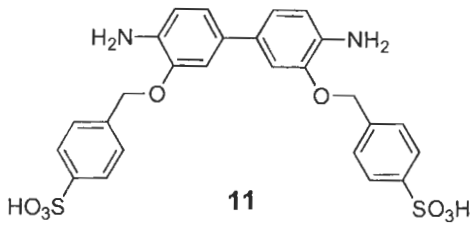

11

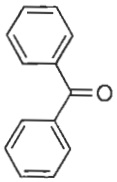

12

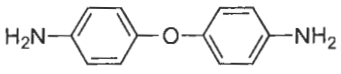

13

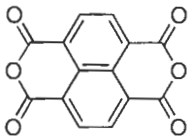

14

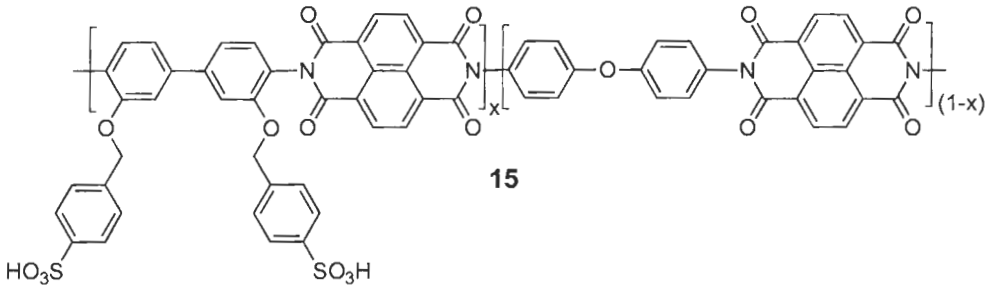

15

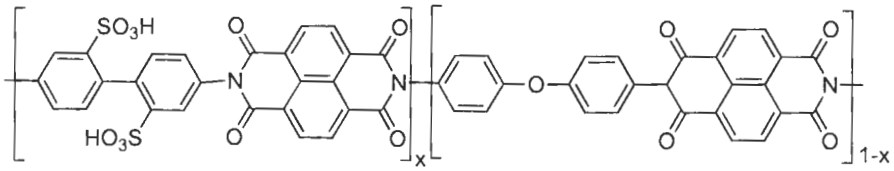

16

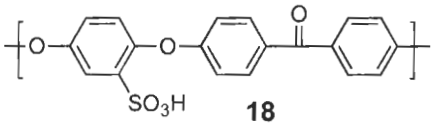

18

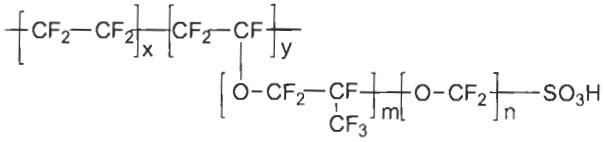

17

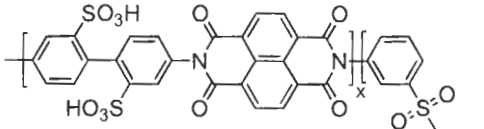

19

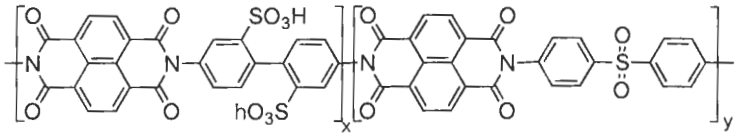

20

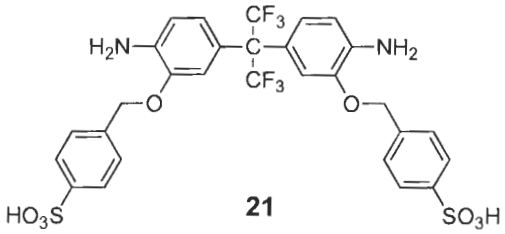

21

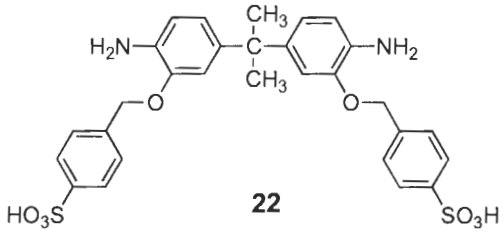

22

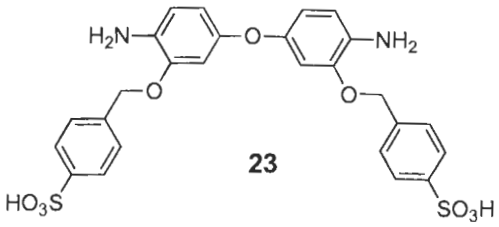

23

CHAPTER 1: INTRODUCTION

1.1 Fuel cell technology

1.1.1 History

The main factor that made the discovery of fuel cell possible was the invention of the chemical pile by Alessandro Volta in 1800. This opened the way to the first demonstrated electrolysis of water in 1800 by Nicholson and Carlyle. As will be explained later, the electrolysis of water is the reverse reduction reaction of the H_2/O_2 fuel cell. Even though the reactions are closely related, it took nearly 40 years to report that "reverse" electrolysis reaction could produce electricity from hydrogen and oxygen. Schoenbein was the first one to publish results related to the fuel cell effect in the *Philosophical Magazine* in 1839.[1] Indeed, after water electrolysis with platinum electrodes in a dilute sulphuric acid solution, he noticed that he could measure voltage/current between the two electrodes.

The first actual demonstration of a fuel cell was by William Grove in 1839.[2] In this paper, published a month after Schoenbein's, he described his experiments with two platinum electrodes immersed half in acidified water and half in hydrogen and oxygen respectively.[2] These experiments demonstrated that the opposite reaction of water electrolysis produces electricity. In 1842, he published his first paper about a working fuel cell (see Figure 1).[3] This fuel cell consisted of platinum electrodes immersed in dilute sulphuric acid.

More than 40 years later, the first scientific paper using the term "fuel cell" was written by Ostwald.[4] Then, with the invention of the combustion engine in the 1850's, almost all fuel cell research stopped due to the relatively low cost and simplicity of the former technology. One hundred years later, NASA used fuel cell technology to produce emission-less electricity and water for their Apollo mission.

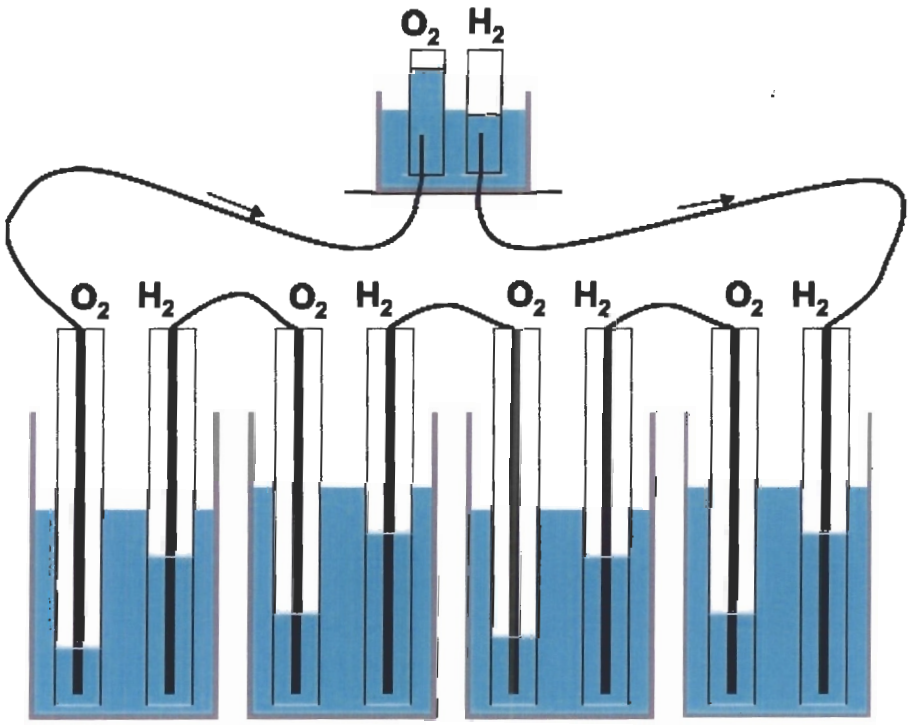

Figure 1: First working fuel cell

The first applications of fuel cell were stationary. Small plants were built to produce enough energy to power houses, small buildings and emergency backup for hospitals and buildings.[5]

Now, with the energy crisis, global warming and the increase of smog in large cities, there is a need to find a clean source of energy to reduce and to limit dependence on fossil fuels.

Examples of clean energy technologies include hydroelectricity, wind power and solar power, but these are mostly for stationary applications. Now, the urgency is automotive power. The electric motor is a good candidate to replace the combustion engine, but batteries have severe drawbacks such as short range for one charge and long charge time.[6] In two decades, efforts were directed to fuel cells for automotive power.[7]

There are many advantages to use fuel cells as a source of electricity. There is a short "recharge" time, therefore autonomy is not a problem.[8] There are no greenhouse or toxic gases emitted if pure hydrogen is used. When pure hydrogen is used, the only product is water. Figure 2 shows the reactions at the anode, cathode and the overall reaction.[7, 9-11] Also, the theoretical efficiency of a fuel cell engine could be much higher than the normal combustion engine.[10, 11] Due to its limitation by Carnot's law of thermodynamics, the combustion engine is restricted to a maximum thermodynamic efficiency of less than 40% under perfect conditions. For fuel cells, 40-70% efficiency is predicted.[12]

Anode: $H_2 \longrightarrow 2H^+ + 2e^-$

Cathode: $1/2O_2 + 2H^+ + 2e^- \longrightarrow H_2O$

Overall: $H_2 + 1/2O_2 \longrightarrow H_2O$ + electric energy + heat

Figure 2: General reactions in a H_2/O_2 fuel cell

There are many types of fuel cells, each have different attributes that make them suitable for specific applications. In transportation and small applications such as cell phones, cameras and laptops, the proton exchange membrane fuel cell (PEMFC) is the most suitable.[9, 13] This is because the operational temperature of PEMFCs is lower than other types of fuel cells and, therefore, it does not require long start up times to reach the right temperature.[14]

PEMFCs, however, have drawbacks that have prevented their commercialization. One is lifetime.[9] For the automotive industry, a fuel cell must last at least 5000 h.[7] Another issue is of the electrode catalyst sensitivity to CO contamination. To reduce the effect of CO contamination, the fuel cell operating temperature should be >100°C. At temperatures lower than 120°C, CO binds to the catalyst, thereby preventing it from performing the necessary electrochemical reactions.[15] By operating above 100°C, the kinetics of both electrodes are enhanced, water management and system cooling will be simplified in addition to dramatically enhancing CO tolerance (from 20 ppm at 80°C to 1000 ppm at 130°C).[16] The solid polymer electrolyte of choice is currently Nafion®. This is based on a fluorinated polymer that possesses a high stability and has a high proton transport efficiency, but its efficiency decreases rapidly at a temperature higher than 80°C.[9, 10, 17, 18]

1.1.2 Types of fuel cell

There are five main types of fuel cells. The main difference is the type of electrolyte used to transport the cations (or anions) from one electrode to the other. This will influence fuel cell characteristics (e.g. operating temperature, type of fuel used, size of the fuel cell) and therefore the principal application. The five main types of fuel cells are: alkaline fuel cell (AFC), solid oxide fuel cell (SOFC), phosphoric acid fuel cell (PAFC), molten carbonate fuel cell (MCFC) and PEMFC.

1.1.2.1 Alkaline fuel cell (AFC)

Reid was the first to describe alkaline fuel cells as early as 1904[14], but it is only in the early 1950s that its viability was demonstrated[14]. The alkaline fuel cell was first used on the Apollo lunar mission. Between 1960 and 1970, they were demonstrated in many more applications such as tractors, cars and boats. Unfortunately for this type of fuel cell, due to reliability (poisoning of electrolyte by CO_2) and safety problems as well as to the later success of PEMFCs, its importance has decreased over the years.

Even if alkaline fuel cells have some problems, this type of fuel cell has some advantages. Because it is much less corrosive than a strong acidic electrolyte, it allows much greater latitude in the selection of electrocatalysts and material of construction. In addition, the conductivity of the alkaline electrolyte is nearly as high as that of a strong acid and KOH is relatively inexpensive compared with other electrolytes.[14] Finally, it is possible to use non-precious

metals, which also reduces the overall cost. Figure 3 represents the operating system of the alkaline fuel cells.

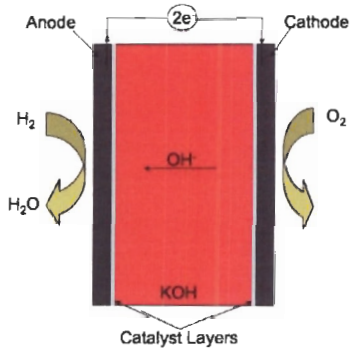

Figure 3: Alkaline fuel cell

1.1.2.2 Solid oxide fuel cell (SOFC)

Solid oxide fuel cells are fuel cells that possess a solid electrolyte composed of an oxide ion-conducting ceramic. Both hydrogen and carbon monoxide can be used as fuel and it is the negatively charged oxygen ion (O^{2-}) that is transported from the cathode to the anode. The most common electrolyte used is zirconia doped with 8 to 10 mole % yttria (Y_2O_3-stabilised ZrO_2). The operating system is represented in Figure 4.

The main advantage of solid oxyde fuel cells is the high operating temperature (1000°C). At this temperature, there is no need for expensive catalysts such as Pt. The fact that the electrolyte is a solid eliminates the problem of leached electrolyte and there is also no need for water management. In principle, different types of fuel (H_2, CO and CH_4) can also be used without the need of a reformer.

The high temperature of operation, however, has important drawbacks. First of all, the materials used have to be very resistant to high temperature and to extreme oxidative and reductive environments. The others problems include: long start-up times, use of brittle heat resistant material, brittle electrolyte and differences in thermal expansion of materials.[19]

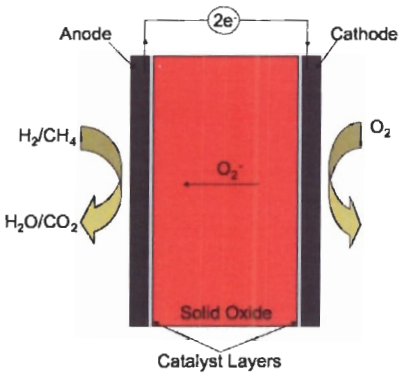

Figure 4: Solid oxide fuel cell

1.1.2.3 Phosphoric acid fuel cell (PAFC)

The phosphoric acid fuel cell is similar to the PEMFC but uses phosphoric acid as the electrolyte. Phosphoric acid is used due to its high thermal, chemical, and electrochemical stability and its low volatility. It is contained within a matrix of silicon carbide by capillary action. An advantage of this electrolyte is its tolerance to carbon monoxide. The operating system of phosphoric acid fuel cell is shown in Figure 5.

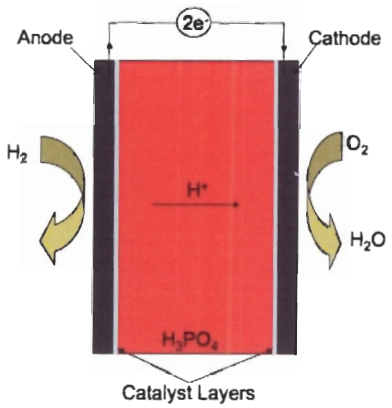

Figure 5: Phosphoric acid fuel cell

Due to the high stability and low volatility of phosphoric acid, the phosphoric acid fuel cell can be operated at high temperatures (150-220°C). The use of high concentration phosphoric acid (~100%) minimises the water-vapor pressure so water management is easy to control.

The main drawback of phosphoric acid fuel cells is that it cannot operate at a temperature lower than 150°C, because phosphoric acid is a poor ionic conductor at low temperature. Another problem is the loss of electrolyte even though the vapour pressure is low. The water produced at the cathode during operation washes out phosphoric acid.[14]

Between 1980 and 1990, multi-megawatt phosphoric acid fuel cells were built and successfully used to provide energy to buildings in Japan by UTC Power (USA). Other power plants of this type were also built around the planet and some companies have already commercialized phoshoric acid fuel cells.[14]

1.1.2.4 Molten carbonate fuel cell (MCFC)

The electrolyte for this type of fuel cell is a molten mixture of alkali metal carbonates. Broers and Letekaar discovered this type of fuel cell in the late 1950s. At its operating temperature (600-700°C), the electrolyte shows high conduction for the carbonate ion (CO_3^{2-}). The biggest difference between this type of fuel cell and the others is the fact that carbon dioxide needs to be supplied to the anode as well as oxygen (see Figure 6).

The main advantage of molten carbonate fuel cells is its high operating temperature. At this temperature, less active catalysts metal can be used, such as nickel. Another one is the fact that the carbon dioxide produced at the cathode can be recycled and reused at the anode. It can also use carbon monoxide as fuel.[19]

There are, however, some disadvantages with molten carbonate fuel cells. The most significant is the fact that it is hard to find materials that can contain the molten carbonate electrolyte at this temperature; therefore, lifetimes of these fuel cells tend to be too short.[19]

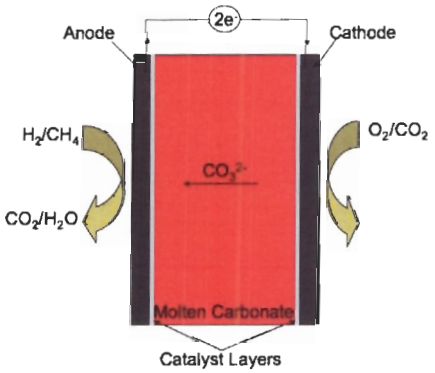

Figure 6: Molten carbonate fuel cell

1.1.2.5 Proton exchange membranes fuel cell (PEMFC)

The first PEMFC was built by General Electric in the 1960s for the NASA Gemini missions. The polymers used at that time (cross-linked polystyrene-divinylbenzene-sulfonic acid and sulfonated phenol-formaldehyde) were relatively unstable to oxidation, having lifetimes <500h. In 1967, Dupont introduced Nafion®. Even today, Nafion® is still the technology standard.

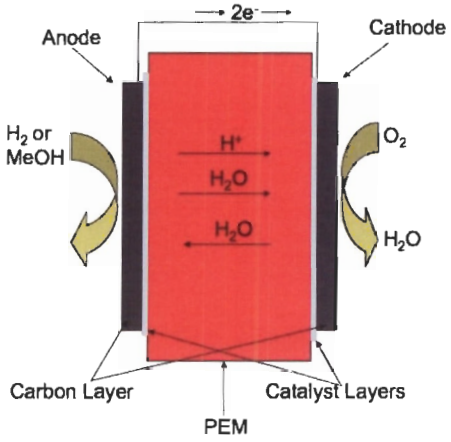

Figure 7: Proton exchange membrane fuel cell

To meet PEMFC requirements, a membrane must be electrically insulating, gas impermeable, resistant to oxidation, hydrolytically stable and posses a glass transition higher than operating temperature.[20] To be proton conductive, PEMFC membranes need to be hydrated. The polymer consists of a hydrophobic backbone containing hydrophilic groups (usually $-SO_3H$). This creates a phase separation in the polymer membrane and leads to the formation of channel-like structures that allows protons to move from the anode to the cathode[21, 22] through these channels via the Grotthuss (Figure 8) and vehicular (water diffusion) mechanism.[22]

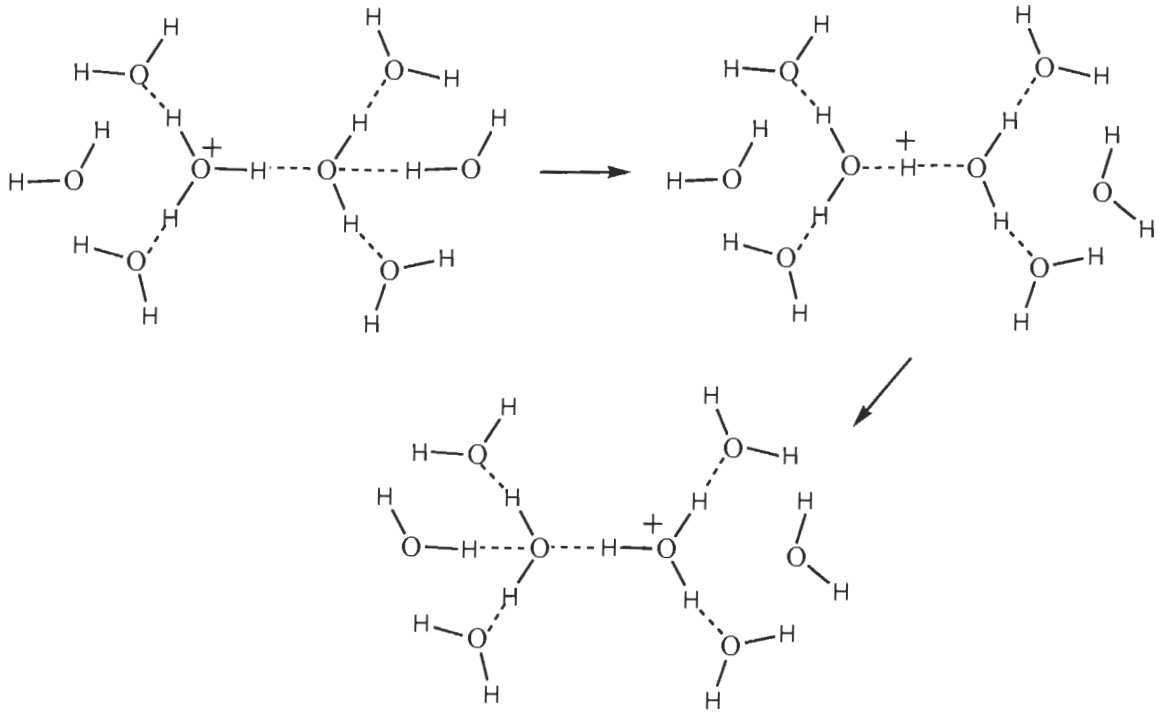

Figure 8: Scheme representing the proposed Grotthuss mechanism[23]

PEMFCs have many advantages that make them attractive for automotive applications. They operate at temperatures <100°C, and thus have a fast start-up time. They are simple, there are few corrosion problems and water is the only by product.[14]

PEMFCs are good candidates for applications such as small electronic devices due to their low operating temperature and their compactness. They last longer per "charge" compared to batteries and can be recharged faster.

There are drawbacks to PEMFCs. Water management is an issue. A dry membrane does not conduct protons and a flooded fuel cell starves the cell of fuel/oxidant. Secondly, the low operating temperatures make them susceptible to CO poisoning. CO contaminates the platinum active sites and reduces the

amount of platinum available for electrochemical reaction.[15] Slightly higher temperatures (~120°C) could help solve this problem.[15] Unfortunately, high temperature (>100°C) operation is difficult since available polymers (including Nafion®) cannot maintain sufficient level of hydration to maintain adequate proton conductivity. Chemical stability at these temperatures is another issue.[16]

A need exists to find alternatives to Nafion®. Alternatives can be classified into four categories: fluorinated, post-sulfonated hydrocarbons, directly sulfonated hydrocarbons, and acid-base complexes.[7, 9, 10] Of all these materials, hydrocarbon based polymers have been the most intensively studied due to the wide variety of these polymers that are available and the fact that it is easier to synthesize and modify most of these polymers.[7, 9] Polyimides in particular are a class of polymers that have the potential to be used in fuel cells due to their high chemical, thermal and oxidative stability.

CHAPTER 2: LITERATURE REVIEW

2.1 PEMFC membranes

There are many characteristics that PEMFC membranes need to have to be good candidates for fuel cell applications. These include: high proton conductivity, low permeability to fuel and oxidant, low electronic conductivity, good water transport, oxidative and hydrolytic stability, good mechanical properties and capability to be assembled into a membrane electrode assembly (MEA).[9] Unfortunately, none of the existing membranes can satisfy all of these criteria. This is at least in part due to the fact that the relationship between the microstructure of a PEM and its resulting properties is still not fully understood.

Many different polymers have been investigated for fuel cell applications. These polymers can be divided into four main categories: perfluorinated, post-sulfonated, directly sulfonated and acid-base complexes.

2.1.1 Perfluorinated polymers

Currently, the most widely-used membrane in PEMFC is Nafion®. It was first made by Dupont in 1962 and was originally designed as a separator in chlor-alkali production. It consists of a polytetrafluoroethylene backbone and regularly spaced perfluorovinyl ether pendant side chains terminated by sulfonic acid groups (see Figure 9). It is known for its high chemical and thermal stability due to its fluorinated backbone. This very hydrophobic backbone is also responsible

for the high conductivity of Nafion®. The large polarity difference between the backbone and the hydrophyllic side chain increases the phase separation. This leads to better interconnection between hydrophilic parts to form a better ionic network, and this allows Nafion® to possess a high proton conductivity (around 0.1 S/cm) for a relatively small number of sulfonic acid groups.[22, 24]

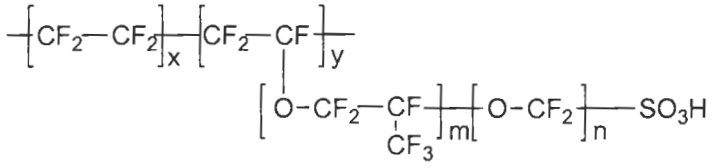

Figure 9: Nafion® structure

The highly hydrophobic backbone increases the phase separation with the sulfonate groups located at the end of the side chain. Many groups have studied this characteristic and many models have been developed to explain this behaviour.[18, 22, 25] It was found that, at a certain concentration, the hydrophobic parts agglomerate leaving the hydrophilic parts outside to form a channel type network.[26]

Other companies have tried to improve Nafion® by changing the structure of the monomers. Nafion®-like membranes include: Flemion® (ASAHI Glass), ACIPLEX® (ASAHI Chemical) and DOW XUS® (Figure 10). Still, Nafion® remains the membrane of choice in commercial PEMFC applications.

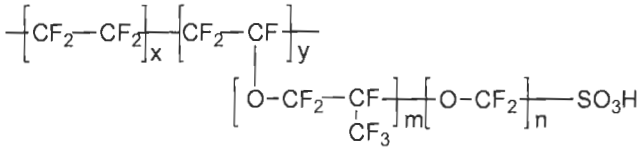

Nafion m≠ 1, n=2, x=5-13, y=1000
Flemion m=0, n=1-5
Aciplex m=0, 3, n=2-5, x=1.5-14
Dow Membrane m=0, n=2, x=3.6-10

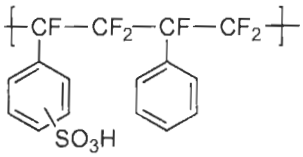

Linear Sulfonated poly(trifluorostyrene)

Figure 10: Other perfluorinated polymers

The problems of Nafion® and similar membranes are their low conductivity at high temperature (>80°C). They are susceptible to dehydration and, therefore, decreased conductivity. Also, their low mechanical strength at high temperature is a major drawback.[9] Other membranes are being investigated for PEMFCs.

2.1.2 Post-sulfonated polymers

A large number of different polymer systems have been investigated as replacements for perfluorinated PEMs. After some modification, many polymers, usually composed of aromatic groups, can be converted to proton conducting membranes. The post-sulfonation method is the easiest way to obtain a proton conducting polymer for these systems. An advantage of this route is the potential to use commercially-available polymers. By using sulfonating agents, it is possible to add sulfonic acid groups onto the aromatic rings (Figure 11 gives one example of post-sulfonation). The number of SO_3H groups on the polymer chain depends on reaction time and temperature. This dependence gives the possibility to control different properties of the membranes. The problems with this method, however, are the lack of precise control over the degree and

location of functionalization and the possibility of side reactions or degradation of the polymer backbone.[9]

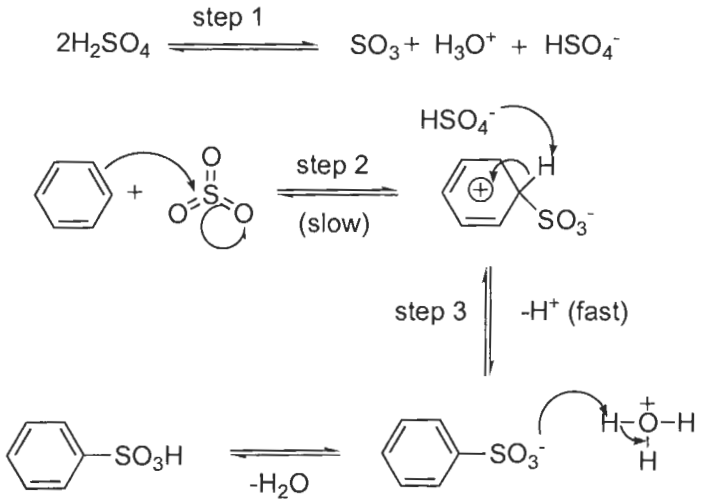

Figure 11: Example of post-sulfonation mechanism

Different sulfonating agents can be used for post-sulfonation e.g., sulphuric acid, chlorosulfonic acid, sulfur trioxide-triethyl phosphate complex. Sulfonation is an electrophilic substitution reaction and the presence of ring-activating groups (e.g. NH_2, OH) or ring-deactivation groups (NO_2, CN) will either favour reaction the reaction or not.[27] It is also important to know that the sulfonic acid group is usually restricted to the activated positions on the aromatic ring.

The polymers normally used are polyarylenes, poly (arylene ethers), polyimides (PI), polyetherimides, poly (aryl ether ketones) (PAEK) and poly sulfones (PSu).

2.1.3 Directly sulfonated polymers

Due to the drawbacks of postmodification methods, other techniques have been used to synthesize PEMs. One of these methods is the use of sulfonated monomers whereby it is possible to control the position of the sulfonic acid group on the aromatic rings. Other positive aspects include the possibility to control the molecular weight (although the molecular weight of bare polymers used in the post-sulfonation can be controlled, the post-sulfonation can degrade the polymer backbone) and to insert different monomers to change the properties of the polymer. Direct sulfonation can be used as a route to many of the same systems obtained via post-sulfonation such as poly (ether ether ketone), poly (arylene ether sulfone), polysulfone and polyimide.

The first reported sulfonated monomer was made by Robeson and Matzner[28] for use as a flame retardant. More recently, Ueda et al. reported the synthesis of 3,3'-disulfonated-4,4'-dichlorodiphenyl sulfone[29] which has subsequently been demonstrated in a fuel cell by McGrath et al.[30] Figure 12 shows the synthesis of this monomer.

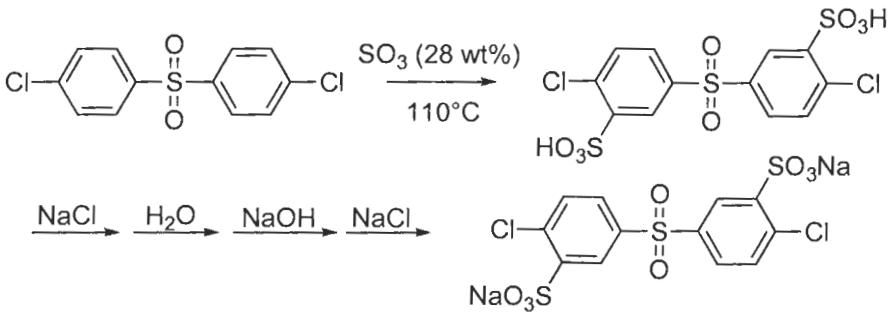

Figure 12: Synthesis of 3,3'-disulfonated-4,4'-dichlorodiphenyl sulfone

The sulfonation degree of these polymers can be controlled by changing the ratio of sulfonated/unsulfonated monomers. Figure 13 shows an example of one of these polymers.

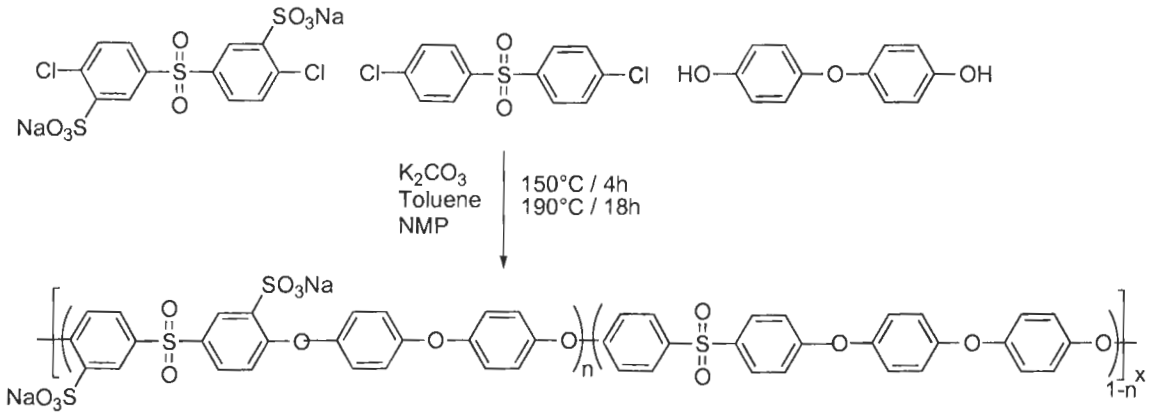

Figure 13: Example of directly sulfonated polymer

As for other sulfonated polymers, these systems exhibit a hydrophilic/hydrophobic phase separated morphology that changes depending on the degree of sulfonation. As expected, water uptake, ion exchange capacity and conductivity increase when the sulfonation degree increases. With this technique, it is possible to change the membrane properties by changing the

monomers used and not only by changing the sulfonation degree as in post-sulfonation.

2.1.4 Polymeric acid-base complexes

Other ways to potentially improve existing membranes or the synthesis of other type of polymers have also been investigated; such as acid-base complexes. There are other systems that have been studied such as: polymer blends and doped membranes. However, only acid-base complexes will be discussed here because it is the most similar with the work described in this thesis.

One of the most studied examples in this category are the acid-base complex systems. These systems involve incorporation of an acid into an alkaline polymer to promote proton conduction. They seem to be a good alternative for membranes so as to maintain high conductivity at elevated temperature. The most studied polymers for this type of system is poly(2,2'-(m-phenylene)-5,5'-dibenzimidazole) (PBI) (see Figure 14). These polymers can be doped with different acids (usually H_3PO_4). Instead of being dependant on humidity levels like classical PEMs, their conductivity is dependant on the doping level[10]. The doping level is the molar percentage of acid per repeat unit of the polymer. By changing the doping level from 450% to 1600% it is possible to raise the conductivity from 4.6×10^{-2} S/cm to 0.13 S/cm (165°C).[10] Another advantage of this type of PEM is its capacity to operate at high temperature (T>100°C), as its performance is not related to the humidity of the membrane.

Unfortunately, the long-term stability of these systems in fuel cell application is still yet to be proven.

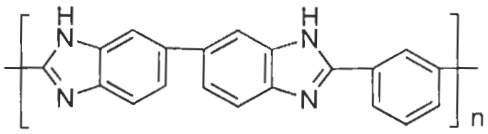

Figure 14: Example of poly(2,2'-(m-phenylene)-5,5'-dibenzimidazole) (PBI)

Reynolds et al. also used PBI as a proton exchange membrane, but in this case they carried out a post-sulfonation by adding a sulfonated side chain.[31] An advantage of this method is the control of the position of the sulfonic acid groups. The sulfonated side chains are attached to the nitrogen bearing a proton prior to lithiation. This technique can be considered as a post-sulfonation method, but with the sulfonic acid groups on a side chain instead of on the backbone. Glipa et al. first introduced a sulfonated side chain on PBI.[32] They introduced sodium (4-bromomethyl)benzenesulfonate as a side chain in order to increase the solubility of PBI as well as to make it proton conductive. They were able to obtain conductivity values of 10^{-4}-10^{-2} S cm^{-1} at room temperature. Figure 15 shows the sulfonation reaction they used. Karlsson et al. also published details on a similar type of post-sulfonation[33] in which they introduced a sulfonated side chain on polysulfone by sulfination. Figure 16 shows the reaction sequence they used.

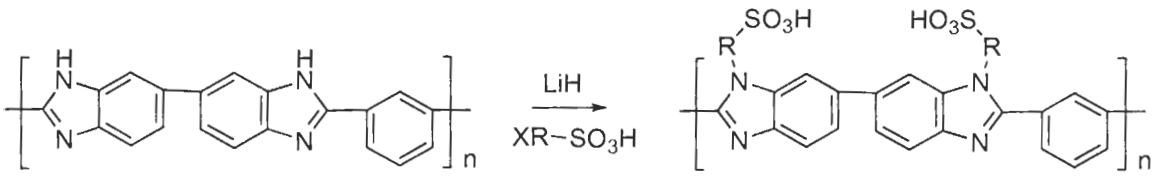

Figure 15: PBI sulfonation

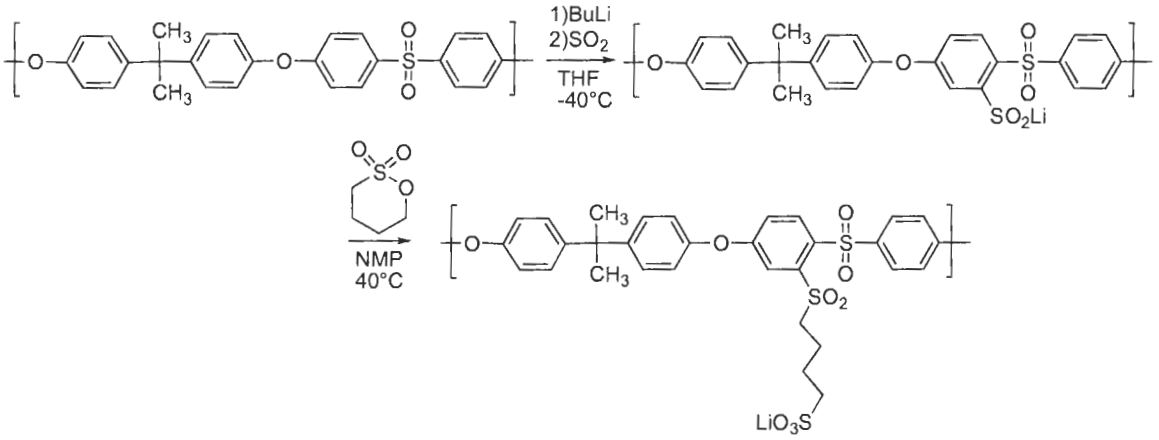

Figure 16: Sulfination example

Another method that has been investigated is the incorporation of submicron particles of metal (IV) phosphates in polymer matrices to increase their proton conductivity. This technique could offer some advantages such as the increase of hydration at high temperature, and the increase of proton conductivity. This method is still relatively unexplored.[10]

2.2 Polyimides

The first aromatic polyimides were produced by Bogert in 1908 through polycondensation of either the ester or the anhydride of 4-aminophthalic acid.[34] In 1955, high molecular weight polymers were synthesized by two-stage polycondensation of pyromellitic dianhydride with a diamine. Since then, many other polyimides have been synthesized. Interest in this type of polymer is due

to their superior thermal and chemical stability as well as their non-flammability.[35] The main applications of polyimides are in electronic, electrical engineering and aviation materials.[35, 36] More recently, they have been used for gas permeability and gas separation as well as having attracted the attention of the fuel cell community.[37-39]

Sulfonated polyimides (sPI) are thought to be good candidates for fuel cell applications. First, their vitreous backbones do not swell as much as other polymers (depending on external conditions) due to the lack of polymer chain mobility to permit the structural rearrangement required for water uptake (e.g., sulfonated polyimides typically exhibit only small dimensional changes with increasing water uptake).[37] They also possess a high polymer glass transition that would be useful for relatively high temperature operation.[38, 40] At first, sulfonated phthalic polyimides (Figure 17a) were used in fuel cells, but they were found to degrade quickly. It was then found that naphthalic polyimides (Figure 17b) are chemically more stable.[41] Further analyses have determined that the phthalic imide structure is more susceptible to hydrolysis than the naphthalenic imide, thus making the latter more suitable for fuel cell application.

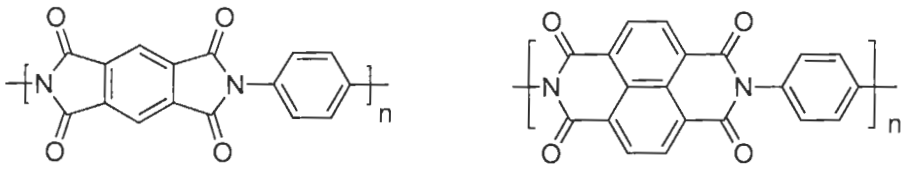

Figure 17: Phathalic (a) and naphthalic (b) imides

The stability of five and six-membered ring sulfonated polyimides was studied by Genies et al. using model compounds.[42] Two models were used for

this study (Figure 18). The first model, composed of sulfonic acid-containing phthalic imide (a), was compared to a second model composed of sulfonic acid-containing naphtalinic imide (b).

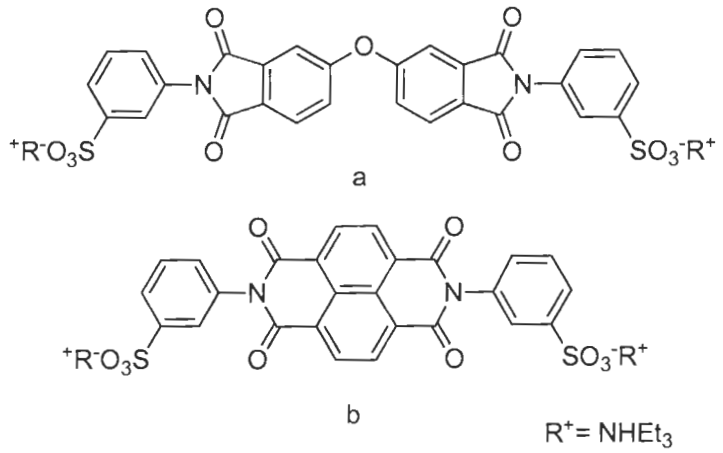

Figure 18: Sulfonated polyimides models

When aged in distilled water at 80°C, it was found by NMR (^{1}H and ^{13}C) and FTIR that the naphthalenic model (b) was stable for 120 h versus 1 h for the phthalic model (a). This is mainly attributed to the strained five-membered imide moieties.[41] The NMR and FTIR analysis have led to the development of a possible degradation mechanism for phthalic and naphthalenic sulfonated polyimides. These results suggest that an equilibrium occurs between the starting material and the product in the naphthalenic model (Figure 19), limiting conversion to the hydrolysis products to only ~12%.[9]

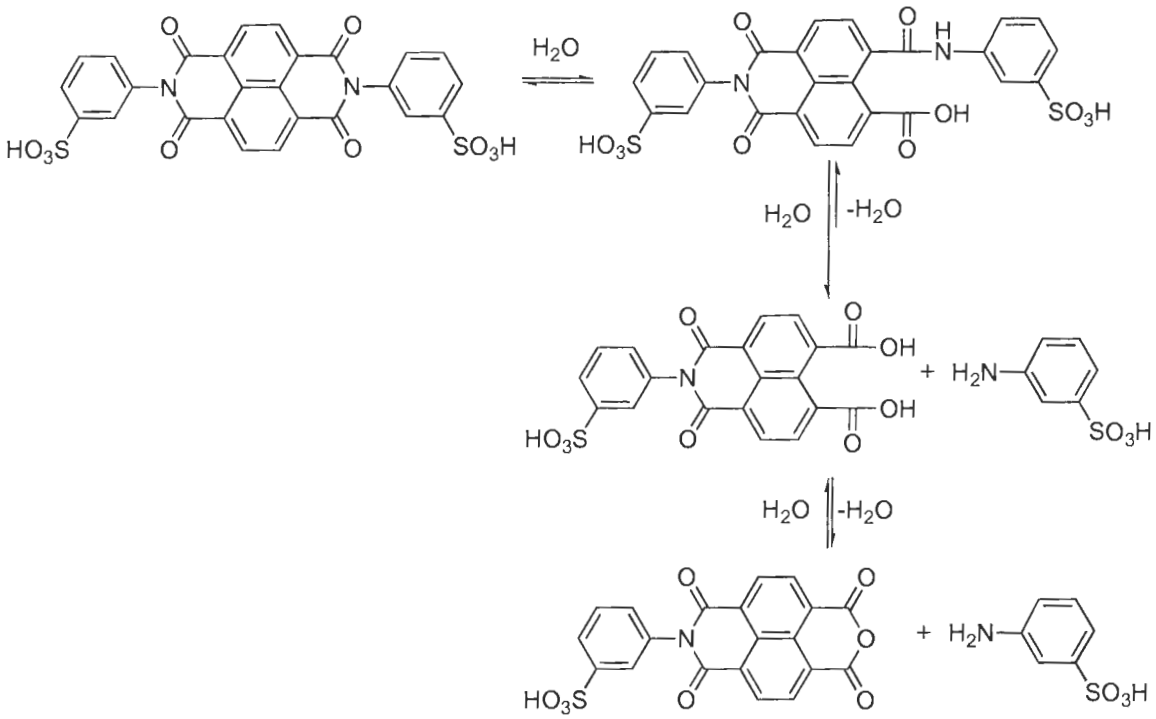

Figure 19: Equilibrium for hydrolysis of naphthalenic sulfonated polyimides

Although hydrolytically more stable than the five membered ring derivative, six-membered ring polyimides exhibit poor solubility.[43] To improve solubility, Genies et al. introduced ether linkages into the main chain and/or bulky groups as substituents. The synthesized polymers were soluble enough to cast as membranes. Figure 20 shows some examples of these polymers.

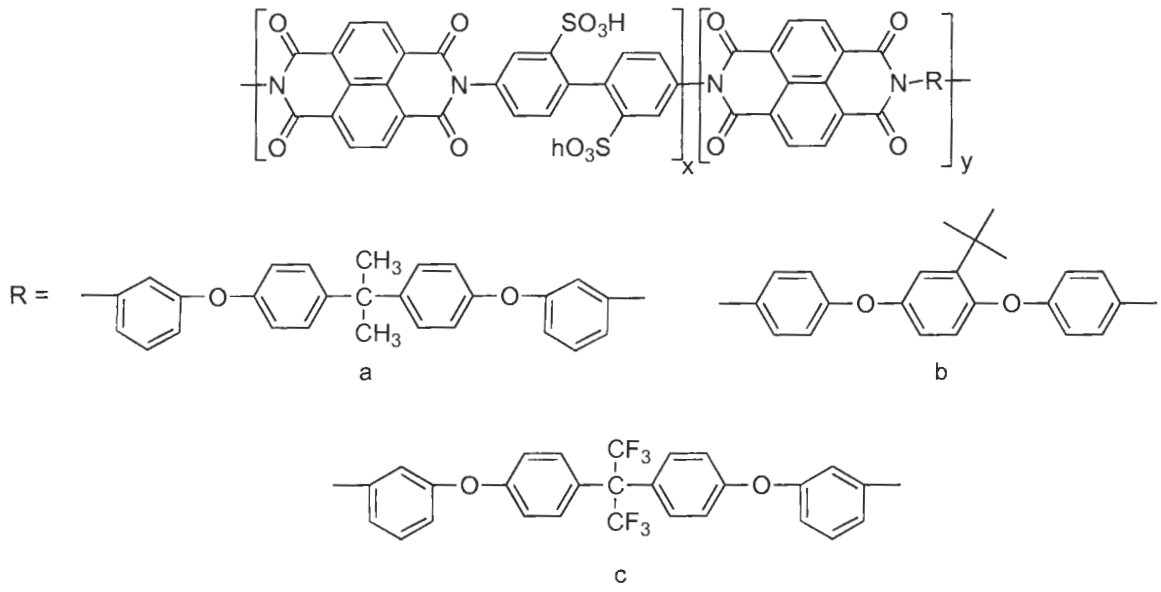

Figure 20: Examples of sulfonated polyimides

With their study, Genies et al. discovered that the solubility of sulfonated polyimides is governed by the nature of the hydrophobic sequence in which solubility is improved by the introduction of phenylether bonds and/or bulky groups in the polymer backbone. Solubility is also increased for polyimides containing meta-amino-substituted diamines in comparison to the para-amino-substituted derivatives. They also found that the random polyimides exhibit better solubility than sequenced polyimides.[43]

Even if the stability was greatly increased for the six-membered rings polyimides, they are generally still too unstable for fuel cell applications. Okamoto et al. were able to increase water stability by synthesizing a sufonated monomer containing an ether bond.[44] Figure 21 gives examples of this polymer. This new polyimide is reported 5 times more stable than the one made by Genies et al.

Usually, the hydrolytic stability of polymers is strongly dependent on the water uptake, which is mainly determined by the ion exchange capacity: the higher the water uptake, the lower the stability. However, with the Okamoto polymer system, water uptake was actually higher for the more stable polymer. These results showed that stability is dependant on backbone flexibility. A flexible chain can undergo relaxation more easily than a rigid one, and this is likely the main reason that sulfonated polyimides containing ether bonds display better water stability.[44]

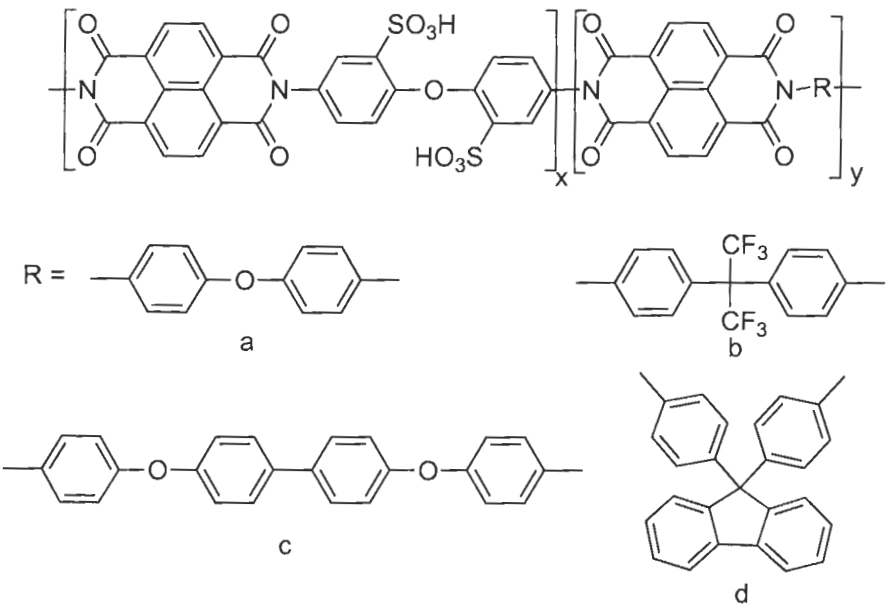

Figure 21: Example of sulfonated polyimides with ether bonds in the main chain

Since the polyimides synthesis reaction is an equilibrium (Figure 22), the water stability of these ones are not only due to backbone flexibility, but also on the basicity of the amine.[34] When the membrane is hydrated during the operation of the fuel cell, the reaction is pushed to the starting material, resulting in ring

opening. An increase in temperature is also an important factor that increases the hydrolysis rate. Therefore, another way to increase the hydrolytic stability of polyimides is to change the basicity of the amine groups.[27, 45]

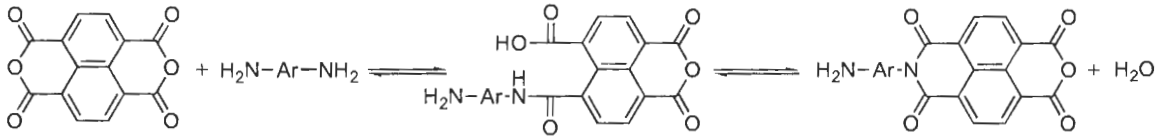

Figure 22: General Example of Naphthalenic Polyimides Equilibrium

Okamoto et al. studied the basicity effect on sulfonated polyimides intended for fuel cell applications.[17, 44, 46-50] By adding the sulfonic acid groups away from the amine groups, they were able to increase the basicity, thus increasing hydrolytic stability. Due to its strong electon-withdrawing power, the sulfonic acid groups decrease the electron density of the phenyl ring and thus the basicity of the amine functionality.[51] By adding this group on a side chain or another phenyl ring, they were able to increase hydrolytic stability. Figure 23 shows some of the monomers they synthesized.

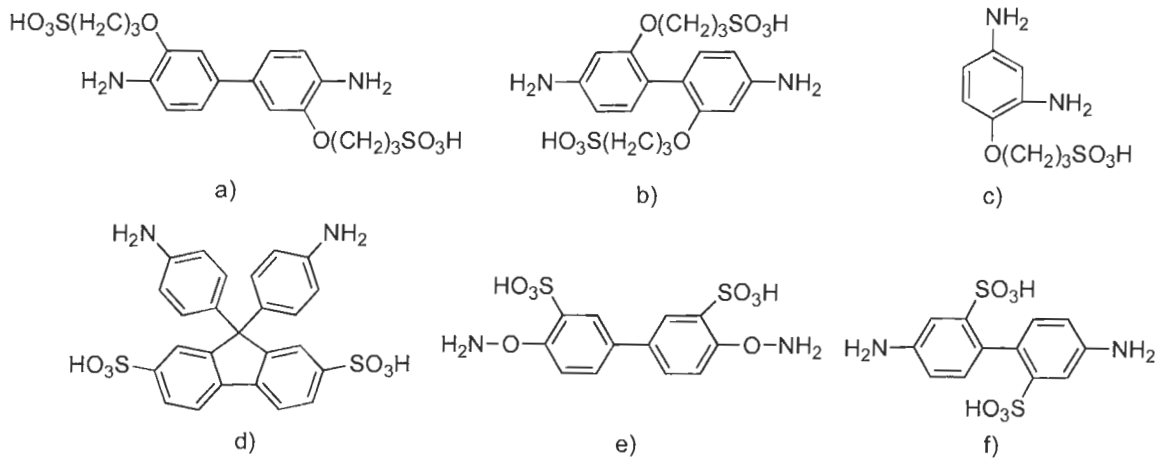

Figure 23: Sulfonated monomers with sulfonated side chains

With these monomers, hydrolytic stability was increased by a factor of 20 for d), 100 for c), 300 for e), 1000 for b) and more than 1000 for a) in comparison with the non-flexible monomer that has the sulfonic acid groups attached directly to the backbone (f).[17, 46, 50]

Increasing the distance between the sulfonic acid groups and the amines also helps to increase hydrolytic stability. Because the hydrolysis of the imido ring is an acid-catalyzed reaction, the protons will be mostly restricted to the ion-rich domains, thus isolated from the polymer main chain and, therefore, hydrolysis of the imido ring of the sulfonated polyimide will be depressed.[46]

2.3 Sulfonated polyimides synthesized in this work

This work focuses on the synthesis of polyimides with the sulfonic acid groups attached to a side chain. It was shown that by adding the sulfonic acid groups on side chains, it is possible to increase the hydrolytic stability of the polyimides and obtain good proton conductivity even at lower water uptake.[40] Indeed, it has been demonstrated that a graft block co-polymer, compared to the

analogous randomly sulfonated polymer, exhibits higher conductivity even at low water uptake.[52]

Three sulfonated side chains (Figure 24) were considered: (4-bromoethyl)benzenesulfonic acid (**1**), 4-chlorobenzenesulfonic acid (**2**) and 3-bromopropanesulfonic acid (**3**). Since **3** was shown by Reynolds to be unstable,[31] it was decided to use one of the other two. **2** is commercially available, but attempts to incorporate this side chain was unsuccessful do to is low reactivity. Side chain **1** was therefore investigated.

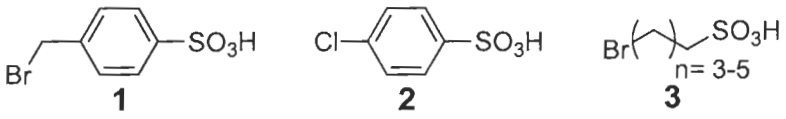

Figure 24: Potential side chains for sulfonated polyimides

By distancing the sulfonic acid groups from the imine functionality, the hydrolytic stability of the polyimide should increase due to the higher basicity of the amine and the increase in degree of phase separation. This was previously demonstrated by Okamoto et al.[17, 47, 50] The main difference between their work and this work is the side chain and the synthetic method used. The method developed in this work allows access to a larger variety of sulfonated monomers, which may lead to sulfonated polyimdes with even better hydrolytic stability. This could be potentially accomplished by using a sulfonated monomer with higher hydrophobicity, e.g., introduction of CF_3 groups and/or greater flexibility such as introduction of an ether bond. These modifications may increase the hydrolytic stability of sPIs further.[40] Sulfonated 3,3'-dihydroxybenzidine was the monomer

used due to its relatively low cost and availability. Other possible sulfonated monomers will be discussed in the conclusion section (Chapter 5).

In order to be suitable for use in a fuel cell, the synthesized polymers must possess high molecular weight and good conductivity as well as hydrolytic and oxidative stability. High molecular weight, important in order to cast membranes with good mechanical properties,[9] was verified by viscosity measurements (see section 3.2.3). We expect that the membranes will have good hydrolytic stability and good conductivity and, more importantly, the method developed in this work will provide the possibility to synthesize different sulfonated monomers that could lead to even greater hydrolytic stability as well as permit further studies on the structure-property relationships of these polymers.

2.4 Goals

The goal of this work was to synthesize novel sulfonated polyimides that will possess a hydrolytic stability that will allow further studies on the structure-property relationships e.g., mechanical properties, proton conductivity, water uptake, hydrolytic stability. Methods reported for preparing grafted polyimides are limited to the use only of a few different types of monomers. The method outlined in this thesis should allow the synthesis of monomers that improve hydrolytic stability of the polyimides. This sulfonated polyimide may also lead to a greater understanding of the relationship between the polymer structure and their properties.

At the time of starting this project, polyimides were considered possible candidates for fuel cell applications.[17, 46, 50, 53] A drawback of polyimides is their potential hydrolytic instability and the resultant deterioration in mechanical properties. Many types of sulfonated polyimides have been synthesized by other groups, but none have yet exhibited the desired stability.[54] It has been previously shown that hydrolytic stability can be increased by increasing polymer backbone flexibility and/or by increasing imine basicity.[40] It is also shown that grafted polyimide may be more stable than a purely linear polymer membranes.[54-56]

CHAPTER 3: RESULTS AND DISCUSSION

This section contains results and a discussion of the synthesized sulfonated polyimides. A description of instrumentation and characterization procedures can be found in chapter 6.

3.1 Synthesis

This section describes the synthesis of the sulfonated polyimides. It includes the synthesis of the sulfonated aromatic side chain, sulfonated monomer and its intermediate product, followed by the series of sulfonated polyimides. Detailed synthetic procedures are provided in Chapter 6.

3.1.1 Sulfonated side chain (4-(bromomethyl)benzene sulfonic acid)

The first compound to be synthesized was the sulfonated side chain (4-(bromomethyl)benzene sulfonic acid). Hubbuch et al. developed this route, using the compound as a protecting group in amino acids synthesis.[57] The same method was used to synthesize the required sulfonated side chain. Section 6.1.1 describes in detail the synthetic procedure. Figure 25 shows the synthesis proposed by Hubbuch et al. [57]

Compound **4** was sulfonated using concentrated sulphuric acid. The proton *para* to the amine was replaced by the SO_3H group to form compound **5**. This electron-withdrawing group has a deshielding effect on the *ortho* and *meta* protons, and moves them downfield (from 7.06 ppm and 7.14 ppm to 7.21 ppm

and 7.53 ppm, respectively). It also has the effect to increase the distance between these two peaks since the protons at the *meta* position are more affected by the electron withdrawing group.

The amine group was then converted to the hydroxyl form to give product **6**. The amine peak (broad singlet at 2.72 ppm) disappeared and was replaced by the hydroxyl triplet at 5.20 ppm. The CH_2 became a doublet (at 4.49 ppm) due to the slowest rate exchange with the hydroxyl group (compared with the amine group)

The final product (**1**) was obtained by converting the hydroxyl group to a bromine. The CH_2 NMR peak was shifted downfield (from 4.49 ppm to 4.69 ppm) and converted to a singlet due to the electron-withdrawing effect of the bromine. The triplet at 5.20 ppm (from the hydroxyl group) also disappeared.

Since this reaction was previously carried out and confirmed by Hubbuch et al., no further characterization was performed on the final product.[57]

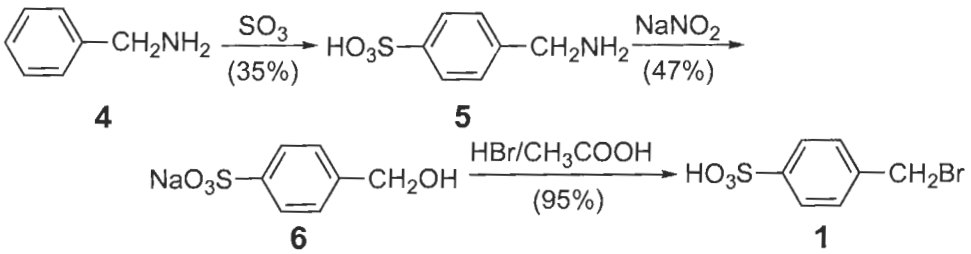

Figure 25: Reaction scheme developed by Hubbuch et al. for the synthesis of 4-(bromomethyl)benzene sulfonic acid[57]

3.1.2 Sulfonated monomer (2,2'-bis(4-sulfobenzyloxy)benzidine)

The next compound synthesized was the sulfonated monomer (2,2'-bis(4-sulfobenzyloxy)benzidine). Different approaches were used. The addition of the

side chain without protecting the amine groups by a S_N2 reaction was attempted. This method was tried with different reagents until it was realized that the amines were too reactive (no primary amine peaks were found in FTIR spectra of the product), thus indicating the necessity for protecting the amine group.[27] The first protecting group used was benzaldehyde. However, even though the protecting reaction worked, it was unstable at high temperature. This was determined using FTIR and ^{1}H NMR, which showed side products (not shown in this work). The exothermic reaction of the deprotonation step (section 6.1.2, 2nd step) might have regenerated the amine. The product was finally determined that benzophenone imine could serve as a good protecting group for the reaction.[58] The side chain reagent was attached to N,N'-bis(diphenylmethylene)-o-aminophenol by a S_N2 reaction and the amines were deprotected via hydrolysis.[59] Figure 26 shows the reaction scheme for the synthesis of 2,2'-bis(4-sulfobenzyloxy)benzidine (**11**). See section 6.1.2 for more experimental details.

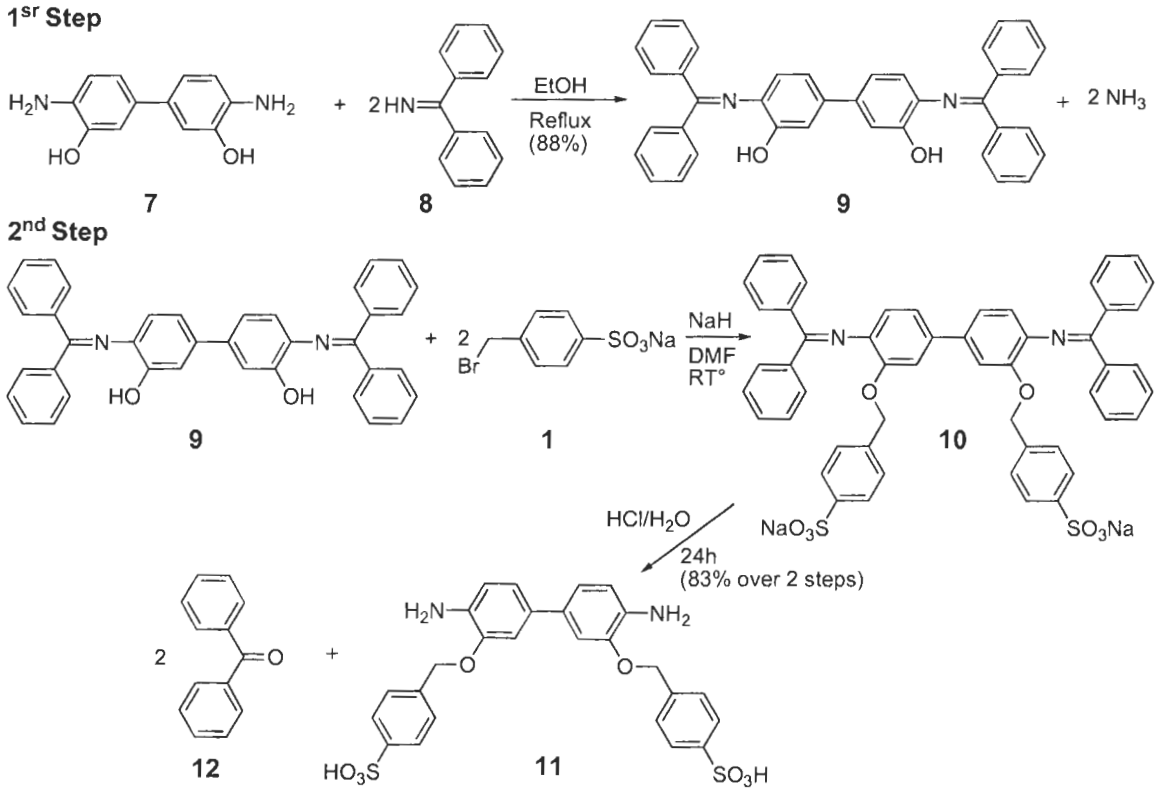

Figure 26: Scheme reaction for the synthesis of 2,2'-bis(4-sulfobenzyloxy)benzidine (11)

The first step was the protection of the amine groups of compound **7** to form **9**. After the addition of **8**, the reaction mixture turned from brown to yellow. No purification was needed to obtain the final product. In the ^{1}H NMR spectrum, the amine peak (4.51 ppm) disappeared and the hydroxyl group remained (singlet at 9.07 ppm). The hydroxyl peak was identified by adding deuterated water to the NMR solution. The fast exchange between the deuterium from the deuterated water and the proton of the hydroxyl group caused the hydroxyl peak to disappear. Figure 27 shows the ^{1}H NMR spectrum of **9**. The integration and positions of the peaks coincide with the expected structure. Figure 28 shows the ^{13}C NMR spectrum of **9**. The number of peaks and their position confirm the

predicted structure. The structure was also confirmed by the presence of O-H (broad peak at 3200 cm^{-1}), C=N (1560 cm^{-1}) and C-N (1323 cm^{-1}) peak in the FTIR spectrum. Results from elemental analysis (C, 83.55; H, 5.39; N, 4.91) were in good agreement with the theoretical composition (C, 83.80; H, 5.18; N, 5.14).

In relation to Figure 27, the singlet at 9.07 ppm is assigned to the hydroxyl group (proved by adding D_2O) Due to the resonance in the Ar-N=C bond, the imine groups cannot rotate freely around the Ar-N bond (due to its double bond character) and thus, the aromatic rings cannot be considered as being symmetrical with the hydroxyl group having a stronger effect on the closest aromatic ring (aromatic ring **a**). The doublet at 7.64 ppm is assigned to the aromatic protons *ortho* to the imine on ring **a**. The triplet at 7.51 ppm is assigned to the proton *para* to the imine on ring **a**. The doublet of doublet (with the appearance of a triplet) centered at 7.44 ppm is assigned to the protons *meta* to the imine on ring **a**. The multiplet at 7.29 ppm is assigned to the protons *meta* to the imine on ring **b** and the proton *para* to the imine on ring **b**. The doublet at 7.16 ppm is assigned to the protons *ortho* to the imine on ring **b**. The singlet at 6.85 ppm is assigned to the proton *ortho* to the hydroxyl on ring **c**. The doublet at 6.68 ppm is assigned to the proton *para* to the hydroxyl group on ring **c**. Finally, the doublet at 6.37 ppm is assigned to the proton *ortho* to the hydroxyl group on ring **c**.

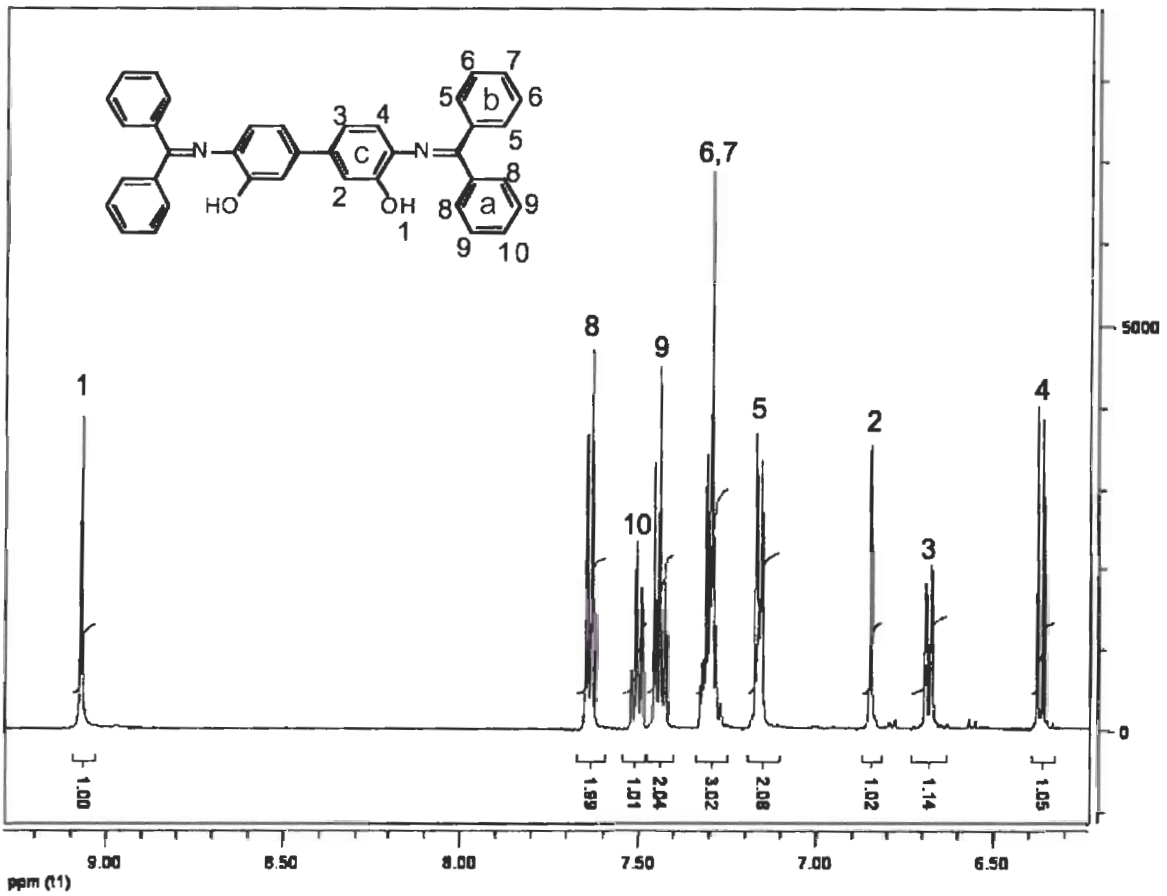

Figure 27: ^{1}H NMR spectrum of N,N'-bis(diphenylmethylene)-o-aminophenol (9) in d_6-DMSO

Figure 28 shows the ^{13}C NMR spectrum of **9**. The peak at 168.19 ppm is assigned to the carbon linked by a double bond in the imine group. The peak at 147.87 ppm is assigned to the carbon linked to the hydroxyl group. The peak at 138.97 ppm is assigned to the carbon *para* to the imine and *meta* to the hydroxyl. The peak at 138.42 ppm is assigned to the carbon linked to the imine and *ortho* to the hydroxyl group The peak at 136.49 ppm is assigned to the carbon linked to the imine on ring **a**. The peak at 135.44 ppm is assigned to the carbon linked to the imine on ring **b**. The peak at 130.78 ppm is assigned to the carbon para to the imine on rink **a**. The peaks at 128.23 ppm are assigned to the carbons *ortho*,

meta and *para* to the imine on ring **b**, and *ortho* and *meta* to the imine on ring **a**. The peak at 120.69 ppm is assigned to the carbon *ortho* to the imine and *meta* to the hydroxyl. The peak at 116.36 ppm is assigned to the carbon *meta* to the imine and *para* to the hydroxyl. The peak at 112.75 ppm is assigned to the carbon *meta* to the imine and *ortho* to the hydroxyl.

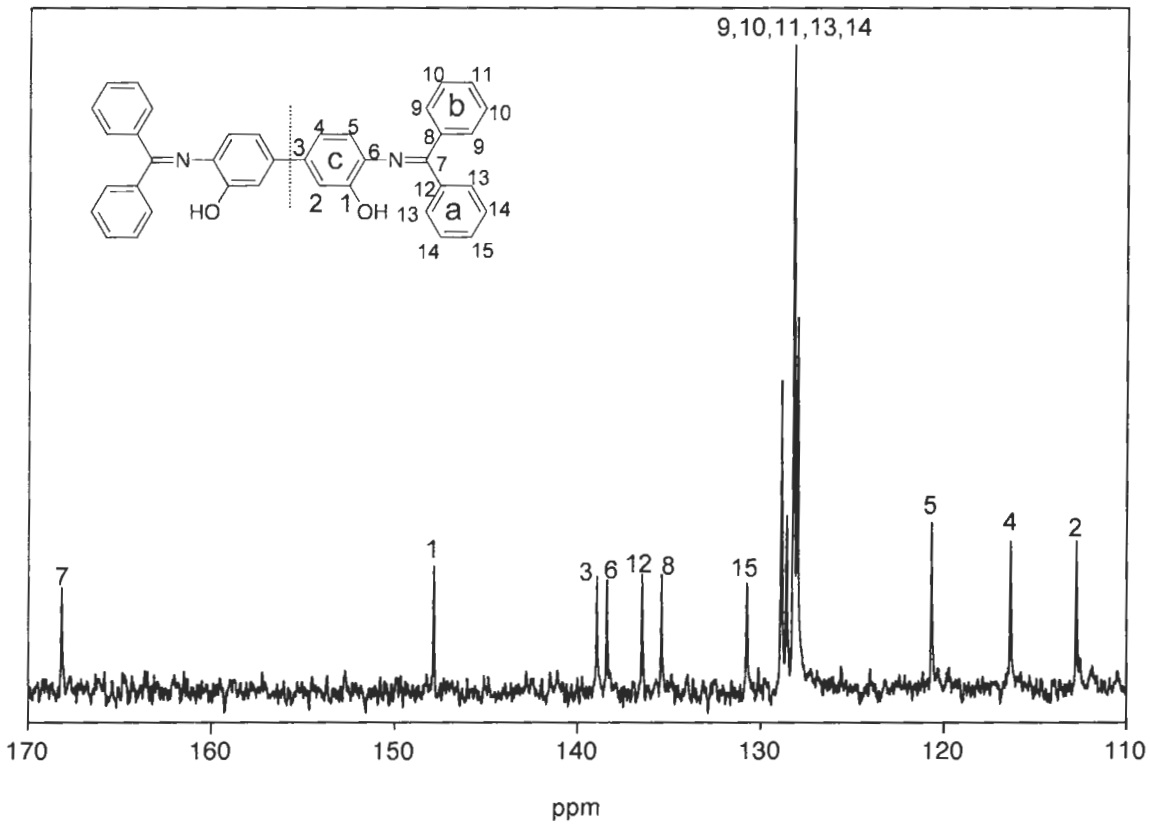

Figure 28: ^{13}C NMR spectrum of N,N'-bis(diphenylmethylene)-o-aminophenol (9) in d_6-DMSO

The second step of the synthesis consists of the addition of the sulfonated side chain (**1**) onto the protected amine (**9**) via a Sn2 reaction. Evidence for the reaction was the change of colour (yellow to red) and the presence of bubbles (from hydrogen formation) during the reaction. The intermediate product (**10**)

was not purified and characterized. The deprotection was carried out via a hydrolyzation of the imine group. The purification of the final product (**11**) is done by precipitation. Compound **11** is soluble in aqueous solution in its salt form and can be precipitated when converted to its acid form. Due to its water solubility, it was possible to remove excess of **1** by multiple washings. The by-product (benzophenone, **12**) formed from the hydrolyzation is a liquid; therefore it was possible to wash it out.

Figure 29 shows the ^{1}H NMR spectrum of **11.** The presence of the amine group (broad peak at 4.68 ppm) is clear. The OH peak (from **9**), as expected, was not present. The spectrum shows the characteristic peaks of the sulfonated side chain (**1**). The doublets at 7.61 ppm and 7.47 ppm are the aromatic protons from **1**. Aliphatic protons are also present at 5.14 ppm. The peak integrals and position are conformed to the predicted structure. Figure 30 shows the ^{13}C NMR spectrum of **11**. The number of peaks and their position are consistent with the predicted structure. The presence of the sulfonic acid group was revealed on the FTIR spectrum with the S=O asymmetric and symmetric stretches at 1238 and 1123 cm^{-1}, respectively. The NH_2 stretch peaks are also present between 3405 and 2621 cm^{-1}. Elemental analysis was also used to confirm the structure. The result obtained (C, 55.89; H, 4.54; N, 4.90) are within an acceptable range from the theoretical composition (C, 56.10; H, 4.35; N, 5.03). The slight difference between the result and the theoretical value may be due to the hygroscopic character of the product.

In relation to Figure 29 the doublet at 7.61 ppm is assigned to protons *ortho* to the sulfonic acid. The doublet at 7.47 ppm is assigned to the protons *meta* to the sulfonic acid group. The doublet at 7.06 ppm is assigned to the proton *meta* to the amine and *ortho* to the ether. The doublet of doublet at 6.89 ppm is assigned to the proton *meta* to the amine and *para* to the ether. The doublet at 6.66 ppm is assigned to the proton *ortho* to the amine and *meta* to the ether. The singlet at 5.14 ppm is assigned to the aliphatic protons. The broad peak at 4.68 ppm is assigned to the protons of the amine.

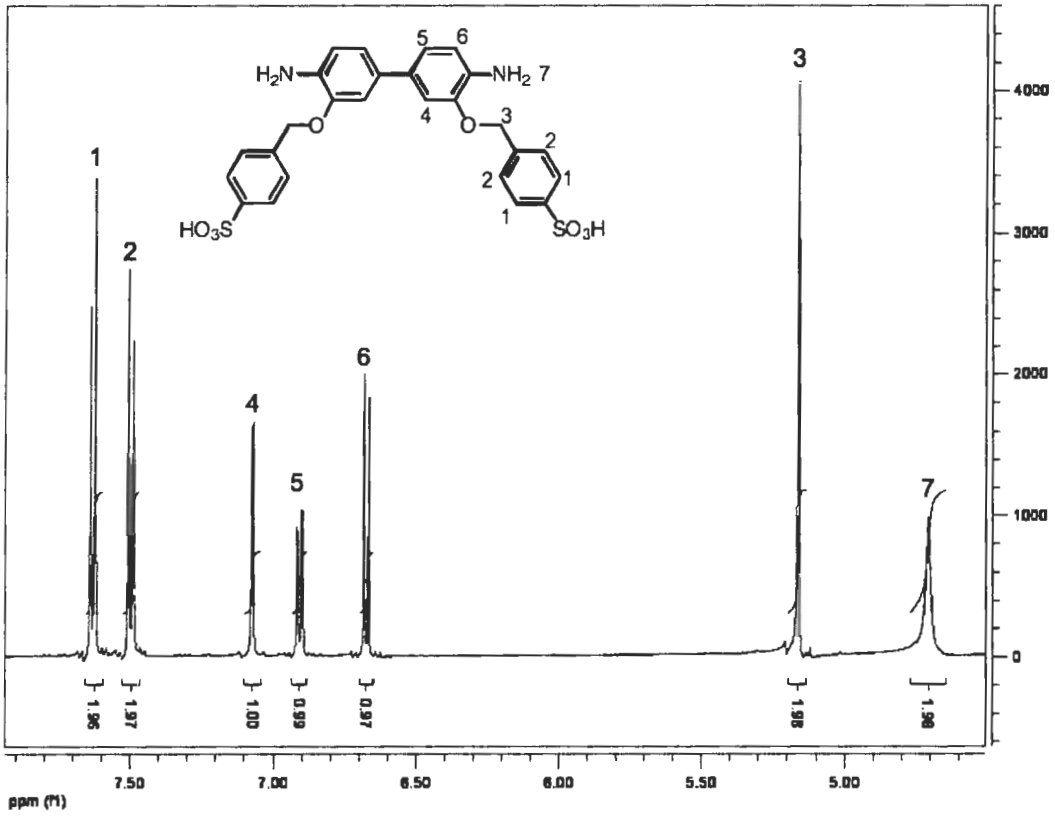

Figure 29: ^{1}H NMR spectrum of 2,2'-bis(4-sulfobenzyloxy)benzidine (11) in d_6-DMSO

In relation to Figure 30, the peak at 152.97 ppm is assigned to the carbon linked to the sulfonic acid group. The peak 150.79 ppm is assigned to the carbon linked to the ether and *ortho* to the amine. The peak at 142.99 ppm is assigned to the carbon *para* to the sulfonic acid. The peak at 141.52 ppm is assigned to the carbon linked to the amine. The peak at 134.74 ppm is assigned to the carbon *para* to the amine. The peak at 132.03 is assigned to the carbons *ortho* to the sulfonic acid. The peak at 130.77 ppm is assigned to the carbons *meta* to the sulfonic acid group. The peak at 123.80 ppm is assigned to the carbon *meta* to the amine and *para* to the ether. The peak at 119.57 ppm is assigned to the carbon *ortho* to the amine and *meta* to the ether. The peak at 115.35 ppm is

assigned to the carbon *meta* to the amine and *ortho* to the ether. The peak at 74.47 ppm is assigned to the aliphatic carbon.

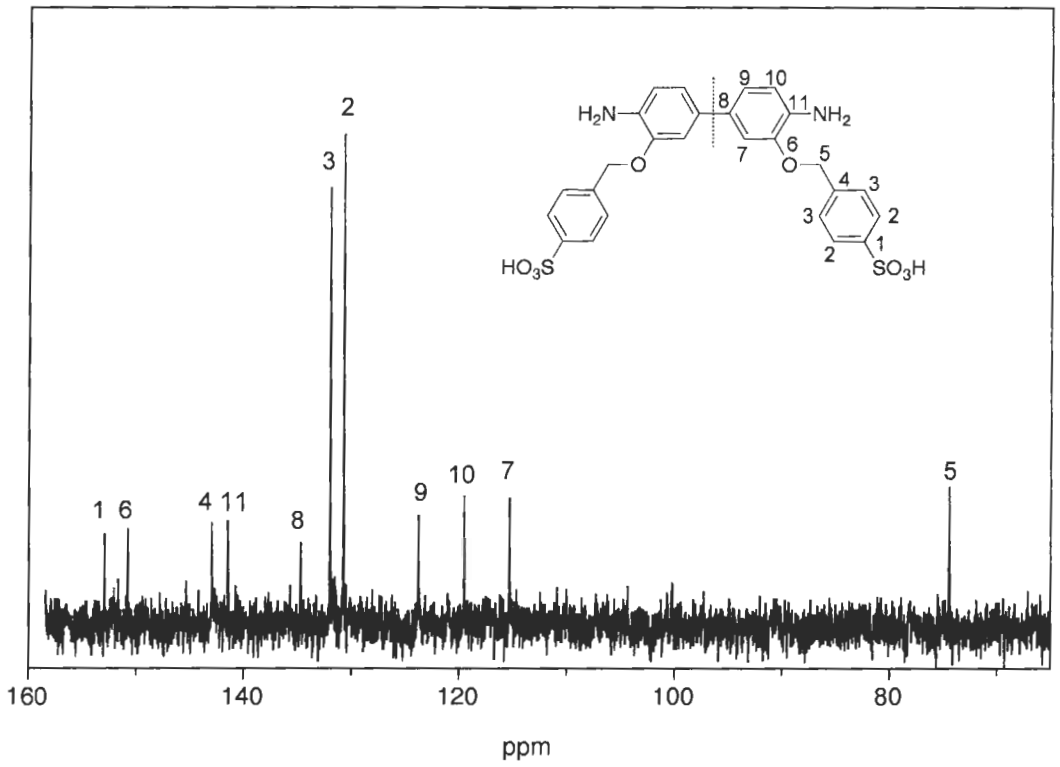

Figure 30: ^{13}C NMR spectrum of 2,2'-bis(4-sulfobenzyloxy)benzidine (11) in d_6-DMSO

3.1.3 Sulfonated polyimides (sPI_X)

The condensation method used for the synthesis of sulfonated polyimides is a well known reaction, and is well describe by Okamoto et al.[49] The polycondensation reaction was performed with different ratios of sulfonated and non-sulfonated monomers (4,4'-oxybisbenzenamine) in order to change the ionic exchange capacity of the polymers. 4,4'-oxybisbenzenamine was chosen because it contains an ether bond which should offer more flexibility to the chain,

thereby increasing hydrolytic stability and its mechanical properties.[44] Figure 31 shows the synthetic scheme for the general reaction.

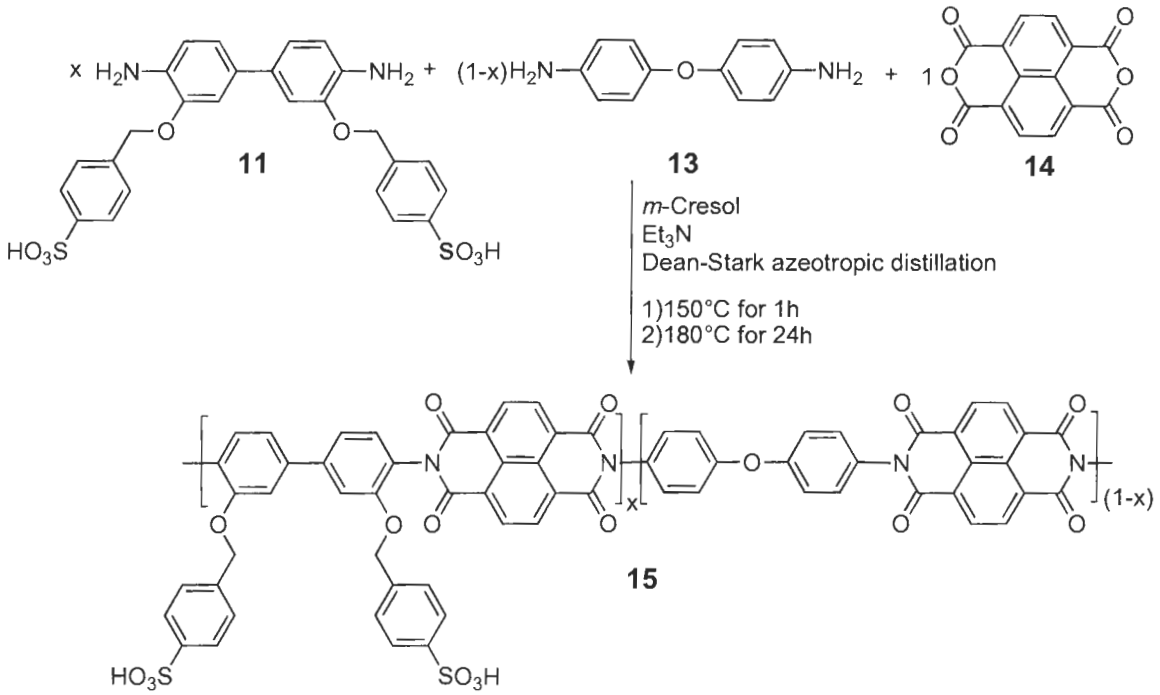

Figure 31: Proposed scheme for the synthesis of the random sulfonated polyimides (sPI_x)

After a few hours of polymerization, the solution viscosity is observed to increase, a sign that polymerization is taking place. Due to the high viscosity of the solution of polymerization, solvent was added prior to precipitation. Figure 32 shows the ^1H NMR spectrum of $sPI_{0.6}$. The other polymers exhibited ^1H NMR having peaks at the same chemical shift except that the integrals between the aromatic and aliphatic protons varied. These results are shown in Table 2. It should be noted that most protons present in the polymer are aromatic in nature. The only non-aromatic protons are those associated with the sulfonated side chain. These protons are located at 5.28 ppm. The aromatic protons of the side

chain are located at approximately the same position found in the ^{1}H NMR spectrum of the sulfonated monomer (**11**) (7.77 ppm and 7.49 ppm). The protons on the naphthalene sections are the most deshielded (8.78 ppm). Protons at the *ortho* position from the imide group (both sulfonated and non-sulfonated parts) exhibit a similar chemical shifts (7.56 ppm). Other protons are situated in the broad peak between 7.39 and 7.22 ppm. The sharp peak at 5.50 ppm is probably due to an impurity. The compound responsible of this peak could not be identified. Due to poor peak resolution, it was not possible to obtain a value for the coupling constant. FTIR was also used to confirm the structure. The presence of the sulfonic acid group was confirmed with peaks of S=O stretch (1123 cm^{-1}), SO_3 symmetric stretch (1037 cm^{-1}) and S-OH stretch (1012 cm^{-1}). Peaks from the imide group are also present (C=O symmetric stretch (1715 cm^{-1}), C=O asymmetric stretch (1675 cm^{-1}) and C-N stretch (1349 cm^{-1})).

Figure 32 shows the ^{1}H NMR spectrum of $sPI_{0.6}$. The peaks at 8.78 ppm are assigned to the protons on the naphthalene structure. The peak at 7.77 ppm is assigned to the protons *ortho* to the sulfonic acid. The peak at 7.56 ppm is assigned to the protons *meta* to the ether and *ortho* to the imide on both the sulfonated and non-sulfonated parts. The peak at 7.49 ppm is assigned to the protons *meta* to the sulfonic acid group. The peaks between 7.39 and 7.22 ppm are assigned to the protons *para* to the ether and *meta* to the imide on both sulfonated and non-sulfonated parts. It is also assigned to the proton *para* to the ether and *meta* to the imide. Finally, the peak at 5.28 is assigned to the aliphatic protons.

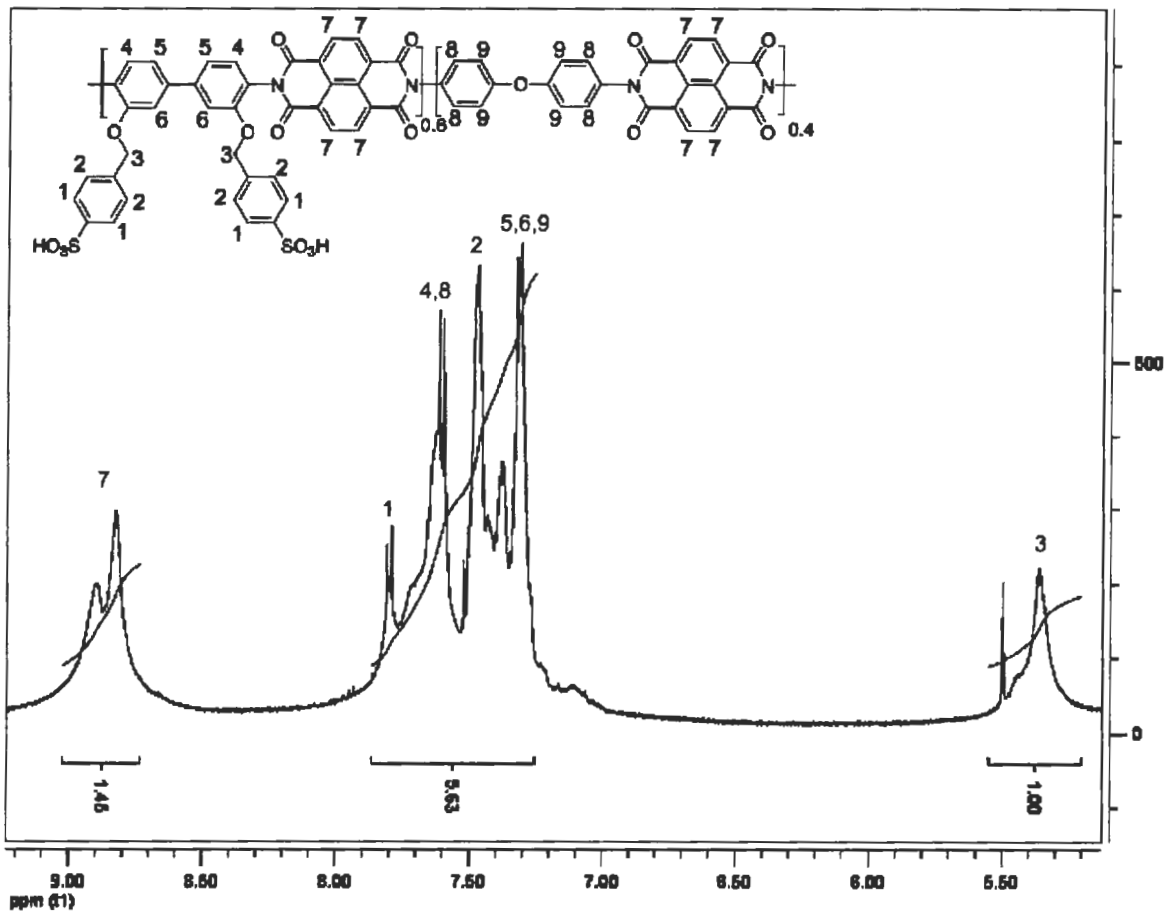

Figure 32: ^{1}H NMR spectrum of $sPI_{0.6}$ in d_6-DMSO

A series of six polymers was synthesized by changing the molar feed ratio (x) of the monomers. The molar feed ratio of sulfonated monomer (**11**) and non-sulfonated monomer (**13**) was changed to obtain different ion exchange capacity (IEC) values. Table 1 shows the nomenclature of the synthesized polymers. As shown in Figure 33, the sulfonated component of the polymer is represented by (x) and the non-sulfonated, (x-1). NMR was also used to calculate the ion exchange capacity (see section 3.3.5)

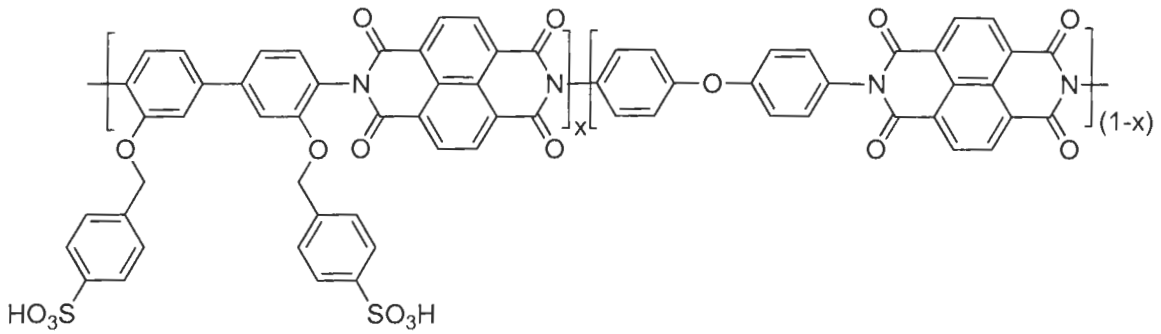

Figure 33: Sulfonated polyimide synthesized in this work containing a sulfonated (x) and non-sulfonated (1-x) section

Table 1: Nomenclature of sulfonated polyimides (sPI_x) based on the feed ratio of sulfonated monomer (x) to non-sulfonated monomer (1-x)

Polymer	x	1-x
$sPI_{0.3}$	0.3	0.7
$sPI_{0.4}$	0.4	0.6
$sPI_{0.5}$	0.5	0.5
$sPI_{0.6}$	0.6	0.4
$sPI_{0.7}$	0.7	0.3
$sPI_{0.8}$	0.8	0.2

Due to the peak proximity and low resolution, it was not possible to get accurate integrations of each peak. To solve this problem, a different approach was used to confirm the polymer structure. The integrations of the aromatic and aliphatic protons (only present in the sulfonated monomer component (x)) were compared to obtain a ratio for aromatic/aliphatic protons. This ratio was compared to that determined by the molar feed ratio to give a good indication of the polymer structure. Table 2 shows the results of each polymer (see section 6.3.5 for detailed calculation). As it can be seen in this table, the ratios obtained experimentally are very close to those predicted from the molar feed ratio. The

experimental ratios vary from 11.72 ($sPI_{0.3}$) up to 5.34 ($sPI_{0.8}$). The differences between the ratios are within 15% error.

Table 2: Ratio between aromatic and aliphatic protons based on the feed ratio (FR) and the results obtained by ^1H NMR.

Polymer	Ratio (FR)	Ratio (NMR)
$sPI_{0.3}$	11.50	11.72
$sPI_{0.4}$	9.00	9.17
$sPI_{0.5}$	7.50	8.55
$sPI_{0.6}$	6.50	7.08
$sPI_{0.7}$	5.79	6.14
$sPI_{0.8}$	5.25	5.34

3.2 Characterization

This section describes the characterization of the sulfonated polyimides.

3.2.1 Differential scanning calorimetry (DSC)

Thermal transitions in a polymer are very important properties for a material because they dictate many of the possible applications for the polymer. Differential scanning calorimetry is an important technique utilized for determining the glass transition temperature and the crystalline melting transition temperature of polymers. The crystalline-melting transition temperature (Tm) of a polymer is the melting temperature of the semi-crystalline domains within the polymer. The glass transition temperature (Tg) of a polymer is the temperature at which backbone segments in the amorphous domains of the polymer attain sufficient thermal energy to move in a coordinated manner. In the region of the glass transition temperature, the polymer will change from a glassy material to a

rubbery material.

There are many factors that affect the glass transition of a polymer. Some of these factors include polymer structure, molecular symmetry, molecular weight, structural rigidity and the presence of secondary forces.[60] The secondary forces may be due to the presence of polar groups that can induce interactions such as hydrogen bonding. For sulfonated ionomer-type polymers, the sulfonic acid group usually has an additional effect. The introduction of sulfonate groups raises the glass transition temperature by increasing bulkiness of the polymer repeat unit, thereby increasing the barrier to rotation of the chains.[26]

Differential scanning calorimetry measurements were performed on three sulfonated polyimides with different ion exchange capacity values ($sPI_{0.3}$: 1.03, $sPI_{0.6}$: 1.73, $sPI_{0.8}$: 2.10). Figure 34 shows the thermograms obtained for three samples with different ion exchange capacity ($sPI_{0.3}$, $sPI_{0.6}$, $sPI_{0.8}$). Differential scanning calorimetry was used to find the glass transition temperature of the synthesized polymers. For a non-sulfonated polyimide, the glass transition is reported to be ~300°C.[36] For a sulfonated polyimide, the Tg should be higher due to the introduction of bulky groups. As reported in the literature, it is not possible to obtain the glass transition temperature due to the decomposition of the product between 200°C and 350°C.[40,61] The decomposition temperature are determined by thermogravimetric analysis as described in section 3.2.2.

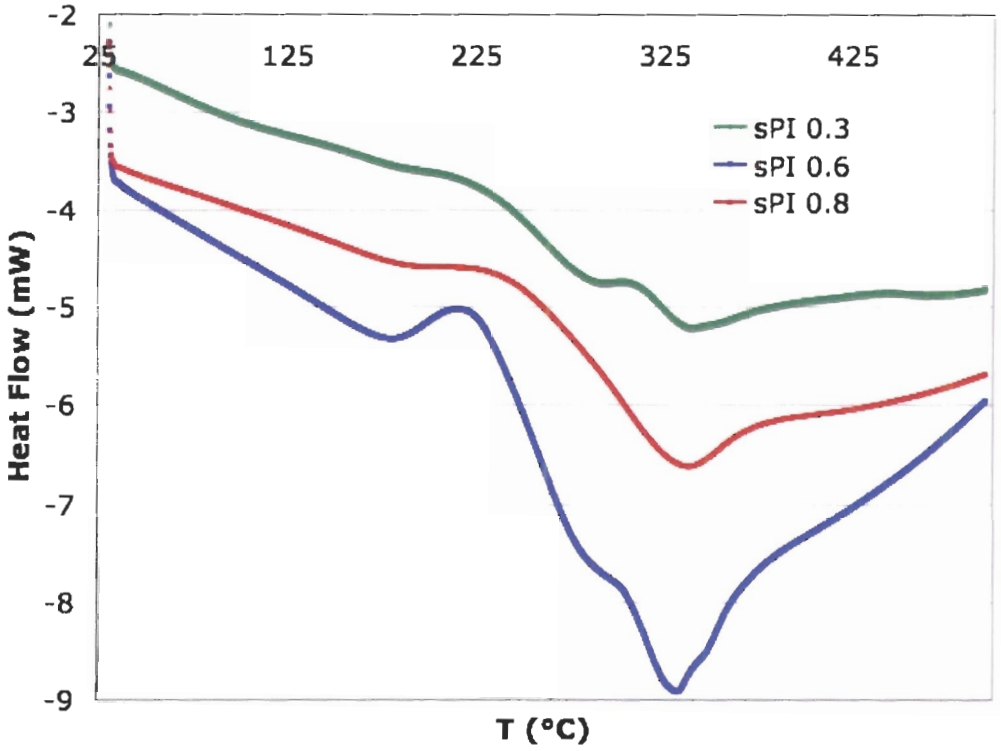

Figure 34: Exothermic thermograms of $sPI_{0.3}$, $sPI_{0.6}$, $sPI_{0.8}$ with IEC of 1.03, 1.73 and 2.10 mmeq/g respectively at a rate of 10°C/min under N_2.

3.2.2 Thermogravimetric analysis (TGA)

The thermal stability of the sulfonated polyimides was determined using thermogravimetric analysis. Thermal stability studies of polyimides have shown that these polymers exhibit a high degradation temperature (~500°C and ~250°C for bare and sulfonated polyimides).[35] Three samples were examined in their acid form. All of the sulfonated samples were pre-heated at 150 °C for 30 minutes in the thermogravimetric analysis instrument furnace to remove traces of solvent and moisture. The dynamic thermogravimetric analysis experiments were then run from 50 to 550 °C, at a heating rate of 10 °C/min under nitrogen.

Thermogravimetric analysis may also give the temperature of desulfonation. It has been previously demonstrated that desulfonation occur at a much lower

temperature than the backbone decomposition.[56] It is also hoped that the desulfonation will be at a higher temperature than when the sulfonate groups are on an alkyl side chain. According to Reynolds et al., the partly aromatic sulfonated side chain has a higher thermal stability than the aliphatic side chain.[31]

Figure 35 shows the thermogravimetric analysis of three sulfonated polyimides with different concentrations of sulfonated monomer ($sPI_{0.3}$, $sPI_{0.6}$, $sPI_{0.8}$). The first loss in mass (at ~220°C) is, according to the literature, due to side chain degradation and desulfonation.[40] It occurs at the same temperature as compared to other sulfonated polymers mentioned in the literature.[48] The second loss in mass (at ~550°C) is due to degradation of polymer backbone degradation since there is change in the slope.[40]

Figure 35 also shows the effect of ion exchange capacity on the thermal properties. The mass loss between 220°C and 375°C (desulfonation) increases as the polymer ion exchange capacity increases. This is due to the higher number of sulfonic acid groups.

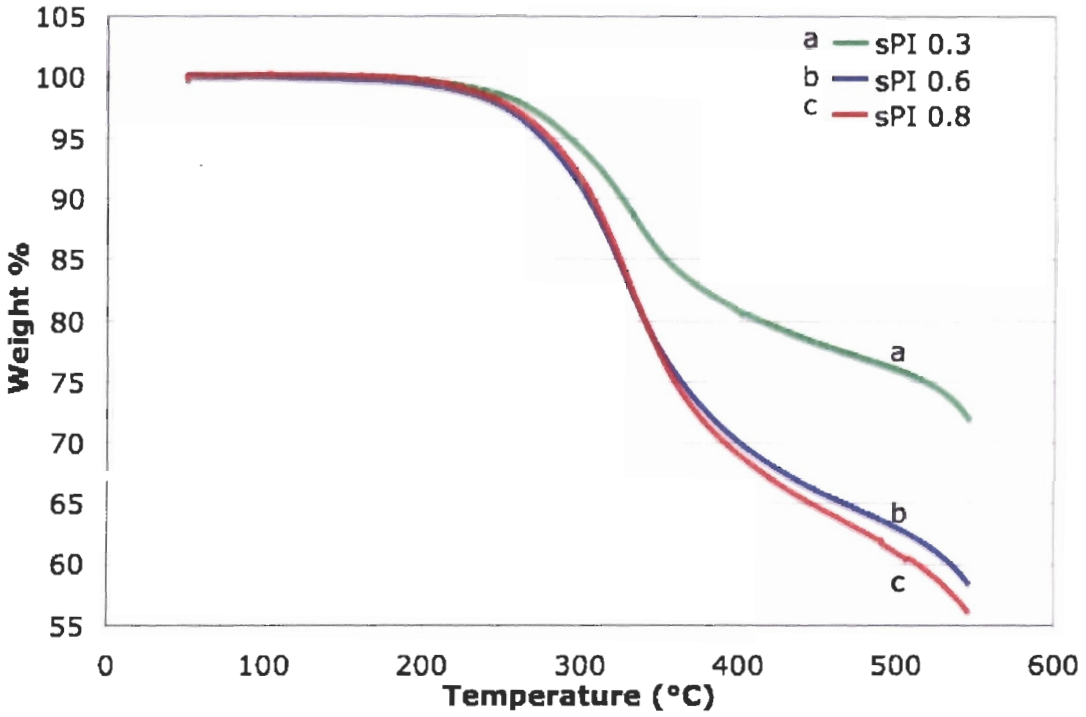

Figure 35: TGAs of $sPI_{0.3}$(a), $sPI_{0.6}$(b), $sPI_{0.8}$(c) with IEC of 1.03, 1.73 and 2.10 mmeq/g respectively at a rate of 10°C/min under N_2.

3.2.3 Solution viscosity

Since the viscosity of a polymer solution is related to molecular weight of the polymer this method was used to give an indication of polymer molecular weight by comparing the results with those in the literature.[62] Because these polymers are ionomers, they behave differently to non-ionic polymers in solution. The reduced and inherent viscosity of strong polyelectrolytes increases rapidly with dilution, instead of decreasing linearly with concentration as is the case for neutral polymers.[63] This phenomenon, the "polyelectrolyte effect", is well documented, and is due to intramolecular and/or intermolecular ionic interactions.[31] As the solution are diluted, the concentration of the counter ions

decreases, forcing ionomer chains to extend (repulsion of anions). This results in an increase of reduced and inherent viscosity.[63]

To avoid the polyelectrolyte effect, two different approaches were used. The first consisted of the addition of 1 wt% LiCl to the DMSO solution in order to counter the polyelectrolyte effect.[31, 64] LiCl was dissolved in water (the smallest possible amount of water) prior to the addition in DMSO due to the insolubility of LiCl in this solvent. Unfortunately, this method turned out not to be applicable, since the polymer precipitated after the addition of the LiCl solution.

The second method used was the one employed by Pineri et al.[43] This method consists of using m-cresol as solvent and triethylammonium as a counter-ion. According to their research, the low dielectric constant of the solvent and large hydrophobic counter-ions mask the effect of electrostatic interactions, which cause the polyelectrolyte effect. This method enabled the measurement of reduced and inherent viscosity (see section 6.3.1) at different polymer concentrations. Unfortunately, a polyelectrolyte effect was still observed even at low concentrations of polymer (Figure 36).[63] This might be due to the fact that not enough counter ions was added to the solution (triethyl amine in this case).

Table 3: Viscosity measurements data for $sPI_{0.6}$ obtained at 30°C in m-cresol with 0.1% (w/w) triethylamine.

[polymer] (g/dL)	t (s)	η_r	η_{inh} (dLg^{-1})	η_{red} (dLg^{-1})
0.6075	53.33	3.934	2.255	4.830
0.4288	40.26	2.970	2.539	4.594
0.3314	34.24	2.526	2.796	4.605
0.2278	28.81	2.125	3.309	4.939
0.1736	26.26	1.937	3.809	5.399
	w_{dry}	0.0729	t_0 (s)	13.56

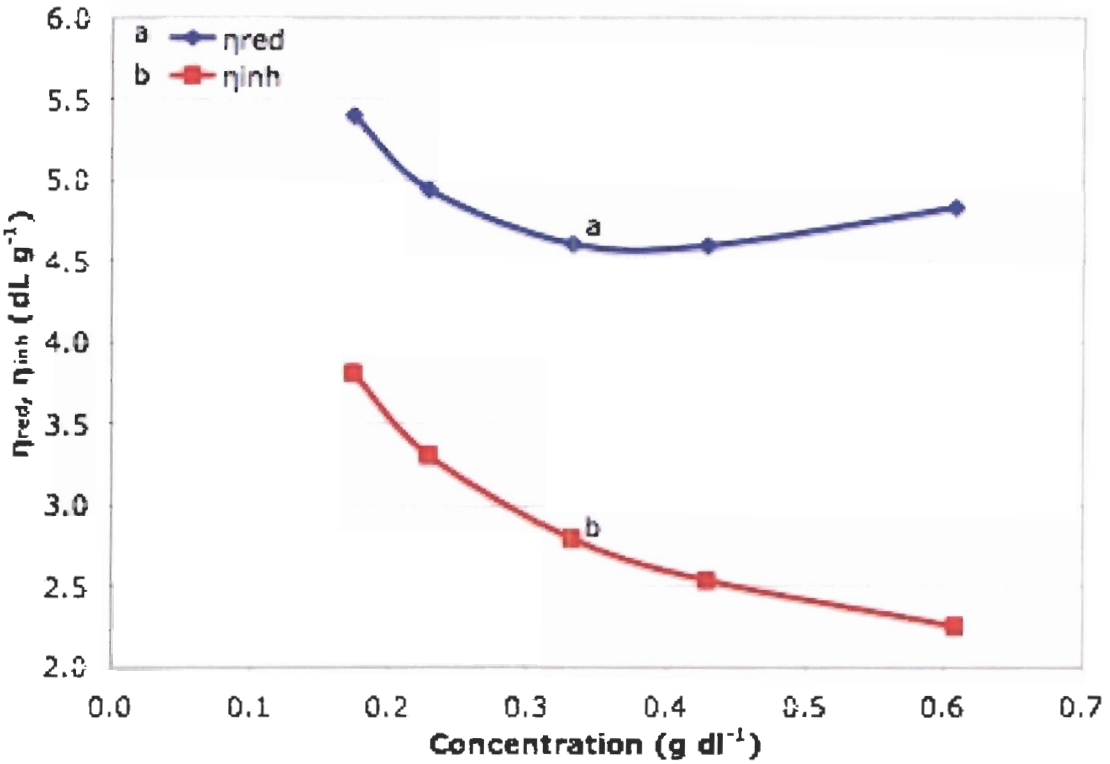

Figure 36: Reduced (a) and inherent (b) viscosity measurements at 30 °C for $sPI_{0.6}$ in m-cresol containing 0.1 wt% triethylamine.

The reduced viscosity results were consistent with those present in the literature. From Figure 36, it was concluded that the reduced viscosity at 0.5 g/dL is 4.7 dL/g. This is in the range of the reduced viscosities for sulfonated polyimides found in the literature at this concentration (2.0 - 7.7 dL/g).[40] Although

molecular weights cannot be extracted from this data, the solution viscosities are consistent with a polymer solution.

3.2.4 Ion exchange capacity (IEC), water uptake (WU) and λ

The ion exchange capacity is a measure of the number of ionic groups (sulfonic acid) per gram of polymer. Ion exchange capacity has a direct influence on membrane properties such as water uptake, swelling, and proton conductivity.

Table 4 shows the experimental ion exchange capacity data obtained by titration, NMR and feed ratio (see sections 6.3.4 and 6.3.5) . These comparisons show good agreement (± 10%) between methods.

Table 4: Ion Exchange Capacity (IEC) based on the feed ratio (FR), NMR and titration for synthesized polymers.

Membrane	IEC (FR) (mmol/g)	IEC (NMR) (mmol/g)	IEC (titration) (mmol/g)
$sPI_{0.3}$	1.10	1.12	1.03
$sPI_{0.4}$	1.38	1.40	1.29
$sPI_{0.5}$	1.62	1.84	1.54
$sPI_{0.6}$	1.83	1.97	1.73
$sPI_{0.7}$	2.02	2.14	1.94
$sPI_{0.8}$	2.19	2.23	2.10

The protonic conductivity of proton exchange membrane is strongly dependant on membrane structure and membrane water content.[22, 37] Increasing the water content helps shield the proton from the negative charge of the SO_3^- groups, thus increasing its mobility.[22] Conversely, decreasing humidity will decrease the proton mobility and hence lower conductivity.

Water uptake, or the level of hydration, is a function of a number of parameters such as: chemical nature of the polymer, temperature, ion exchange capacity, and time required to reach an equilibrium state within the film.[67, 68] The water uptake for the series of the synthesized sulfonated polyimides in this research was determined as a weight percent. The results are shown in Table 5. As expected, the water uptake increases with increasing ion exchange capacity. The increase in ion exchange capacity leads to an increase in the hydrophilicity of the membrane and allows more water sorption.

Table 5: Water uptake (WU) and λ (nH_2O/SO_3H) comparison for membranes at different IEC based on their feed ratio (FR)

Membrane	IEC (FR) (mmol/g)	WU (%)	λ (nH_2O/SO_3H)
$sPI_{0.3}$	1.03	32	17
$sPI_{0.4}$	1.29	35	15
$sPI_{0.5}$	1.54	37	13
$sPI_{0.6}$	1.73	40	13
$sPI_{0.7}$	1.94	53	15
$sPI_{0.8}$	2.10	66	18

The sulfonated polyimides bearing sulfonated side chains generally possess a higher water uptake compared to those sulonated polyimides in which the backbone is directly sulfonated for a similar ion exchange capacity.[40] This might be due to better interconnectivity between ionic domains[67].

However, water uptake is influenced by many parameters: the nature of the non-sulfonated monomer, temperature and even the way membranes are cast can have great influence on the results.[40, 67] For these reasons it sometimes meaningless to compare results with those in the literature. A more hydrophobic diamine will result in a lower water uptake due to the higher hydrophobicity of the

backbone.[69] A non-linear sulfonated polymide backbone possess a suppressed water uptake due to the entanglement of the polymer backbone (see later for more details).[70] Since sulfonated polyimides are glassy polymers with high glass transition values, a change in the casting method (temperature, solvent) will also influence the results.[40]

The number of water molecule per acid group (λ) was also calculated (Table 5), but no trend is observed. These results are contradictory to the values obtained from most membranes. In typical ionomer membranes such as perfluorosulfonated or radiation-grafted membranes, λ generally increases with ion exchange capacity.[43] In the case of sulfonated polyimides, water uptake increases with the ion exchange capacity; however, λ remains almost constant. This surprising result could be explained by a specific morphology of the membranes due to their preparation. The fact that membranes are cast with a specific solvent at a relatively low temperature compared to the polymer glass transition could influence this result.[40]

3.2.5 Volume uptake

Another important characteristic for PEMs is the change in dimension between the dry and hydrated states. Large dimensional changes during hydration-dehydration cycles could increase the stress on the membrane electrode assembly (MEA), leading to a decrease in performance and even cause the MEA to delaminate.[71] The results obtained for the membranes are listed in Table 6.

Table 6: Dimensional change (swelling) of sulfonated polyimides

Dimensions Increase (%)				
Membranes	**Length %**	**Width %**	**Thickness %**	**Volume %**
$sPI_{0.3}$	4.1	8.6	7.4	21.3
$sPI_{0.4}$	11.9	10.3	24.7	53.8
$sPI_{0.5}$	9.5	10.0	19.8	44.2
$sPI_{0.6}$	5.7	5.6	36.4	52.3
$sPI_{0.7}$	9.0	6.6	23.0	42.9
$sPI_{0.8}$	12.8	10.9	45.3	81.6

The results obtained show that there is a relation between the ion exchange capacity and the volume uptake. It is especially obvious for the lowest and highest thickness increase with ion exchange capacities. It also has to be noticed that the change in thickness (21.3 to 81.6 %) is larger than the change in length (4.1 to 12.8 %) and width (8.6 to 10.9 %). Other groups have explained these behaviours by the anisotropic character of this type of polymer.[40, 72] From our results and from what was showed in the literature, it may be that the polymers synthesized have a similar anisotropic character.

3.2.6 Membrane stability

As mentioned before, the polymers synthesized in this work may possess higher hydrolytic stability than linear sulfonated polyimides due to the distancing of the sulfonic acid groups compared to linearly sulfonated polyimides in which the sulfonate is attached directly to the main chain. By having the sulfonic acid on a side chain, the amine basicity is increased and the distance between the hydrophobic (backbone) and hydrophilic (sulfonic acid groups) domains are increased. This should lead to an increase in domain separation and reduces the presence of water near the weakest points.[42]

The hydrolytic stability was evaluated as the time required for the membrane, soaked in hot water, to lose its mechanical properties. The loss of mechanical property was judged to have occurred when the membrane broke after being lightly bent. This method is commonly used for evaluating the stability of sulfonated polyimides.[40]

Five types of membranes were studied: sulfonated polyimide synthesized in this work ($sPI_{0.7}$ (**15**)), Nafion 115 (**17**), sPEEK (**18**) and two other types of sulfonated polyimides made in-house, in which the sulfonic acids were directly attached to the main chain (**19, 20**). All were soaked in 80°C water until they suffer of mechanical failure.

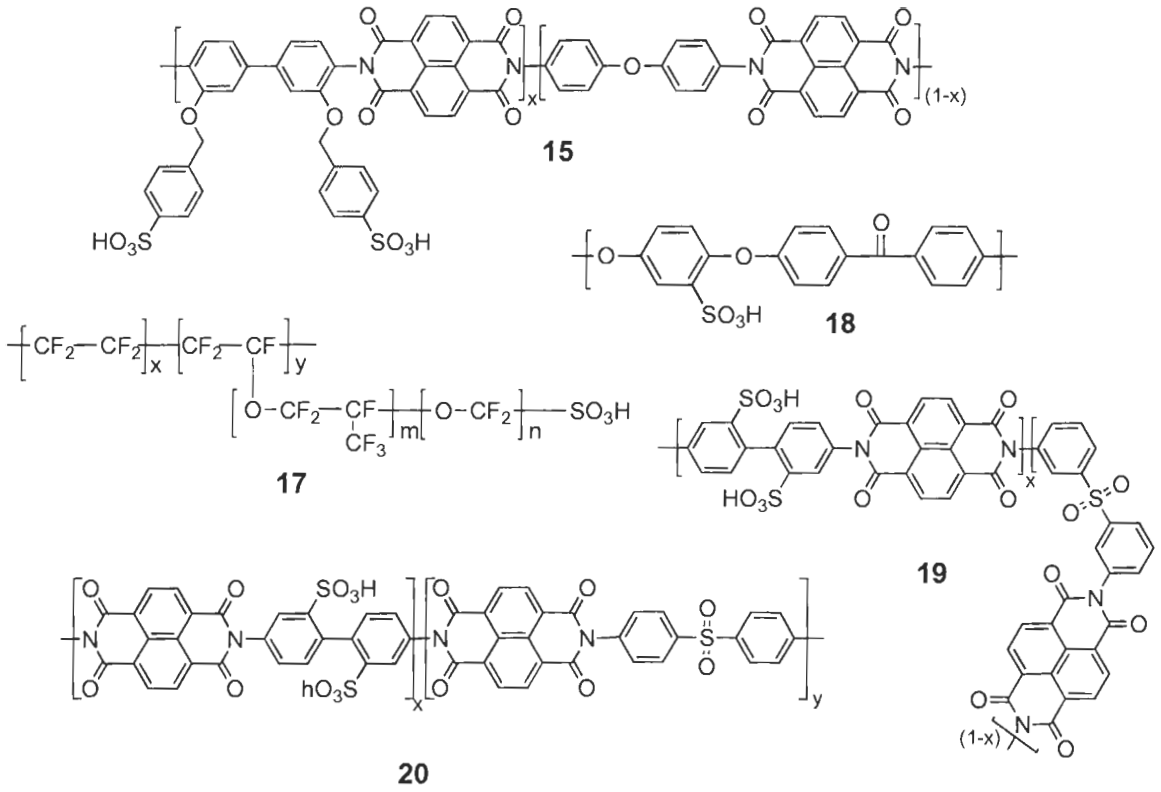

Figure 37: Polymer used to compared the hydrolytic stability (sufonated polyimides (15, sPI), Nafion® (17), sufonated poly ether ether ketone (18, sPEEK), angled sulfonated polyimide (19, a-sPI) and linear sulfonated polyimide (20, l-sPI).

As expected, Nafion® 115 is the most hydrolytically stable; its Teflon® backbone makes it extremely hydrolytically stable and it exhibited no observable loss in mechanical properties offer 120 hours of soaking at elevated temperature. The sulfonated polyimide **15** (synthesized in this work) became brittle after 120 hours. In contrast, the linear sulfonated polyimide (**20**) lost its mechanical properties after < 20 minutes. It is known that these membranes are not hydrolytically stable due to their rigid backbone, relatively low amine basicity of the sulfonated monomer and the proximity of the sulfonic acid to the weakest point of the amine.[40] It also has a high ion exchange capacity and was thinner

than any other membranes (except **15**), which may also account for its instability. The angled sulfonated polyimide (**19**) kept its mechanical properties for two hours due to its lower ion exchange capacity and the fact that it was a thicker membrane.[54] The angled structure might have also influenced the result. Due to this structure, the membrane possesses a lower water and volume uptake, thus less chance of hydrolysis. s-PEEK (**18**), an alternative membrane, was completely dissolved after 20 minutes. **18** is known for its high swelling and lost of mechanical properties in water at high ion exchange capacity.[73, 74]

Table 7 summarizes these results and indicates the main factors (ion exchange capacity and thickness) that can influence the hydrolytic stability of membranes in addition to the polymer structure.[40]

Table 7: Hydrolytic stability at 80°C different membranes with their ion exchange capacity (IEC) and thickness increase

Membrane	IEC (mmol/g)	Thickness (mm)	Time (h)
$sPI_{0.7}$	1.94	0.090	120
Nafion 115	0.97	0.125	>120
sPEEK	2.00	0.103	<0.3
a-sPI	1.80	0.147	2
I-sPI	2.70	0.085	<0.3

3.2.7 Proton conductivity

Conductivity is an important property for investigating the suitability of membranes for PEMFC applications. The magnitude of the specific conductivity is determined by a combination of charge carrier concentration and charge carrier mobility.[22] The charge carrier concentration for PEMs is dependent on the number of pendent sulfonic acid groups along the polymer chain. It also

depends on other factors such as ion exchange capacity, water uptake, acidity of the sulfonic acid groups and membrane morphology.[9] A larger ion exchange capacity leads to a higher water uptake, higher acidity of sulfonic acid groups (i.e. lower pKa) increases proton dissociation and a better phase separation in the membrane will all lead to higher proton conductivity.[40] It should also be recognised that the method of proton conductivity measurement can influence the results. It was shown that in plane proton conductivity gives higher values than through-plane, due to the anisotropic character of sulfonated polyimides.[40]

Figure 38 shows the effect of temperature on conductivity for the series of sulfonated polyimides with Nafion® (N117 for comparison) at 95% relative humidity. It is important to notice that the conductivity increases with the increases of ion exchange capacity ($sPI_{0.3}$ → $sPI_{0.8}$). A constant increase with temperature means that the membrane remains hydrated (e.g. $sPI_{0.8}$). A drop in the conductivity at higher temperature indicates a dehydration of the membrane (e.g. Nafion 117 at 95% relative humidity). An increase of conductivity with the temperature is important for proton exchange membrane applications. As expected, it shows that conductivity increases with temperature and with an increase in sulfonic acid content (IEC). The two curves with the higher conductivity represent the value obtained for N117. They both have the same conductivity value at lower temperature, but the conductivity at 95% relative humidity falls when the temperature increases above 50°C. N117 requires a higher relative humidity (N117 curve at 98% relative humidity) to maintain hydration at higher temperature. It has been suggested that a different

contribution of the proton transport mechanism (Grotthuss and vehicular) could explain the increase in conductivity with temperature phenomenon.[55, 66]

Table 8: Proton conductivity of membranes with different ion exchange capacities at 30°C and 95% RH.

Membrane	W (cm)	t (cm)	l (cm)	R_M (Ω)	σ (S/cm)
$sPI_{0.3}$	0.92	0.027	1.00	3837	0.010
$sPI_{0.4}$	0.91	0.033	0.50	1140	0.015
$sPI_{0.5}$	1.00	0.032	1.00	1322	0.024
$sPI_{0.6}$	0.78	0.005	0.50	4384	0.027
$sPI_{0.7}$	1.13	0.013	1.00	2233	0.030
$sPI_{0.8}$	1.19	0.023	1.00	676	0.053

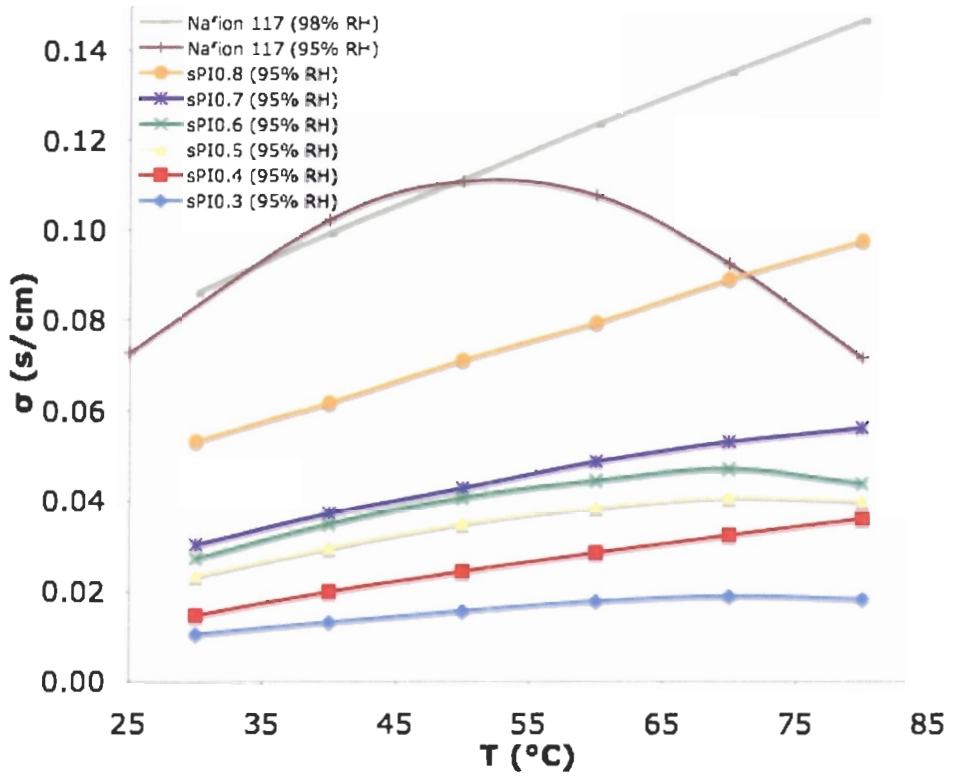

Figure 38: Proton conductivity of Nafion® 117 (95% and 98% RH) and sPI0.3-0.8 (c-h) at 95% RH at different temperatures (30-80°C)

Since most research groups use different procedures for measuring the conductivity (e.g. different relative humidity and/or temperature) it is not always meaningful to compare the results with literature values. It is also difficult to meaningfully compare the effect of the new sulfonated monomer since other groups use different non-sulfonated monomers to synthesize their polymers. However, as mentioned previously, using different monomers changes the properties of the resultant polymer (i.e. flexibility, hydrophobicity and linearity) and this can influence the results (water uptake, swelling, proton conductivity).

An example of a similar structure to the one prepared in this work (**15**) was prepared by Pinéri et al. (**16**) (Figure 39). The difference between these two

polymers is the position of the sulfonic acid. In the Pinéri system (**16**), it is directly attached to the backbone whereas in our case, it is attached to the aromatic side chain (**15**). Another difference is that **16** is block copolymer (with x=5) while **15** is a random copolymer. Also, the backbone rigidity of **16** is due to the absence of flexible bond in the sulfonated monomer block.

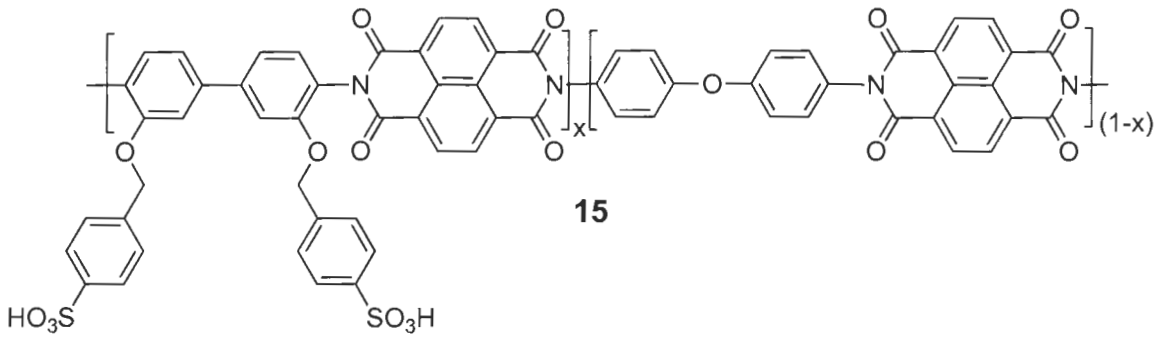

15

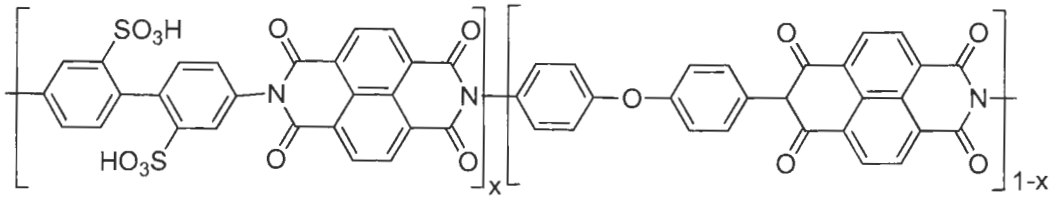

16

Figure 39: Sulfonated polyimides used to compare proton conductivity: sulfonated polyimides synthesized in this work (15) and from Pinéri[37] (16).

It can be observed in Figure 40 that the conductivity of **16** reaches a plateau at lower ion exchange capacity than **15**. This can be explained assuming the existence of highly anisotropic ionic domains with a percolation threshold that requires a lower ion concentration due to the higher rigidity of the backbone of **16**.

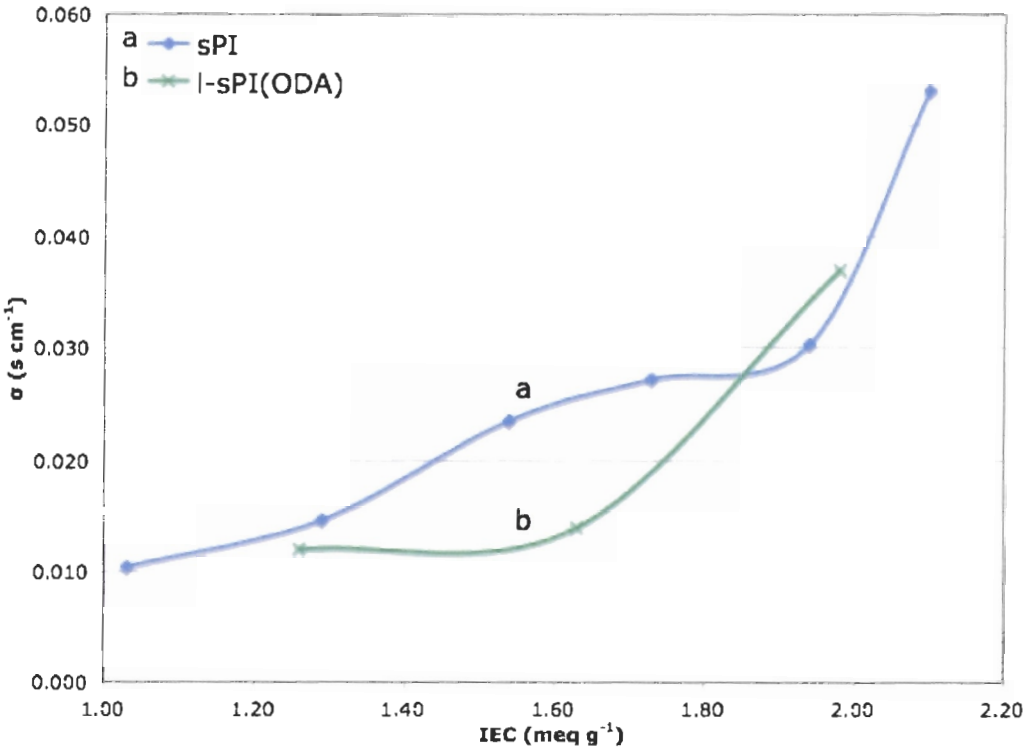

Figure 40: Proton conductivity of 15 (a) and 16 (b) at 30°C and 95 %RH for different IEC (Data (b) taken from: Cornet, N. et al. Journal of New Materials for Electrochemical Systems 2000, 3, (1), 33-42.)

An important result is shown in Figure 41. It shows that the polymer synthesized in this work (**15**) possesses a higher conductivity at the same water uptake than **16**. This can be explained in term of better interconnection between ionic domains, which results from the sulfonated groups. This was also demonstrated for grafted polystyrene system (PS-*g*-PSSA).[75]

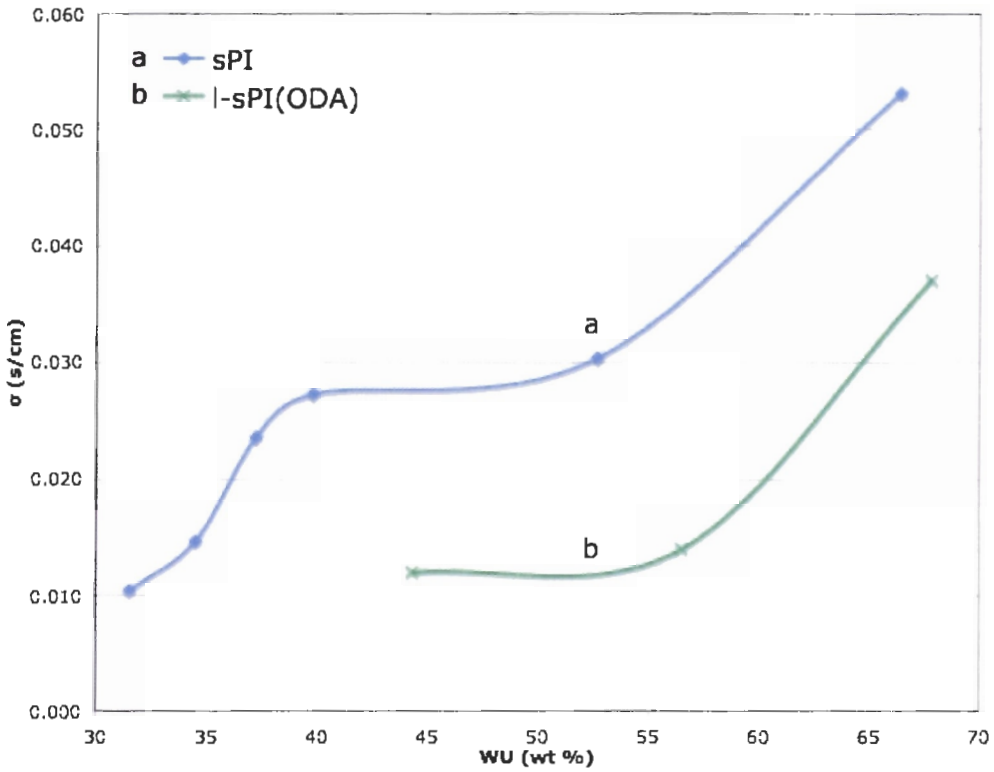

Figure 41: Proton conductivity of 15 (a) and 16 (b) at 30°C and 95 %RH for different WU (Data (b) taken from: Cornet, N. et al. Journal of New Materials for Electrochemical Systems 2000, 3, (1), 33-42.)

3.2.8 Fuel cell test

Figure 42 shows an example of a typical polarization curve for a fuel cell. The initial drop in potential is due to the sluggish kinetics of the oxygen reduction reaction (ORR). The linear drop at moderate current densities is due to Ohmic losses. It is related to the internal fuel cell resistance mainly due to the resistance of the membrane and other components. At high current densities, mass transport losses are observed. Bellow 80°C, most water produced by the ORR is liquid, and it can flood the fuel cell, increasing the resistance to mass transfer (diffusion of O_2 and H_2 through water is slow). Vehicular transport

(electro-osmotic drag) increases this resistance by bringing water to the cathode.[76]

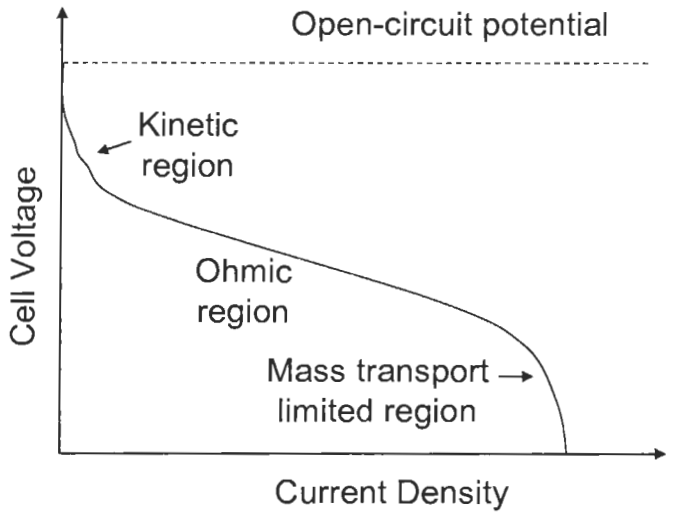

Figure 42: Example of a polarization curve showing losses for a fuel cell

Two different techniques were used to form the membrane electrode assembly (MEA). Hot pressed membranes (HPM) and catalyst coated membranes (CCM) were assembled before testing. Figure 43 shows the polarization curves obtained with Nafion® 115 (CCM (a) and HPM (c)) and $sPI_{0.6}$ (CCM (b) and HPM (d)) at 50°C and fully humidified conditions.

The main regions of interest are the Ohmic and mass transport regions. A steep slope in the Ohmic region is due to a high resistance from the membrane. In both cases, $sPI_{0.6}$ shows a steeper slope compared to Nafion®. With the catalyst coated membrane method, the polarization curves are very similar. The mass transport effect is observed at high current, indicated by a change in the curve of the slope. A mass transport limitation can be observed in the catalyst coated Nafion® and hot pressed Nafion® in fuel cells.

The fuel cell performance of $sPI_{0.6}$ was evaluated. This membrane was chosen because of its good mechanical properties and adequate proton conductivity. Two different assembling methods were used to prepare the membrane electrode assembly (MEA). The hot pressed membrane (HPM) method consisted of assembling the membrane and the separately prepared electrodes by hot pressing them at high temperature (135°C). The second method is called the Catalyst Coated Membrane (CCM) technique; it consists of spraying the electrode (catalyst, carbon, Nafion® solution) directly onto the membrane.

The thicknesses of the membranes used were 30 μm and 35 μm for $sPI_{0.6}$ hot pressed membrane and catalyst coated membrane methods, respectively. Nafion 115 (125μm) and 112 (50μm) were used for hot pressed membrane and catalyst coated membrane methods, respectively. Figure 43 shows the results obtained at 50°C. From this, it can be seen that Nafion 115 performed better than $sPI_{0.6}$ with the hot pressed membrane method. It is important to note that the membrane electrode assembly was not optimized for sulfonated polyimide membranes. Even using high pressure and temperature, the membrane electrode assembly did not bind well due to the high glass transition of $sPI_{0.6}$. Nafion, due to its low glass transition, forms a better interface with the electrodes with the hot pressed membrane method.

The catalyst coated membrane method gave improved fuel cell performance. $sPI_{0.6}$ membrane performed similarly to Nafion 112 at 50°C (even though it possess a lower proton conductivity). This is due to $sPI_{0.6}$ being thinner

than Nafion 112 (35μm vs 50μm). By decreasing the thickness, the membrane's Ohmic resistance is reduced, thereby resulting in a higher performance.[77]

Further investigations will have to be performed in order to obtain a better understanding of the effect of sulfonated polyimides microstructure effect on fuel cell performance.

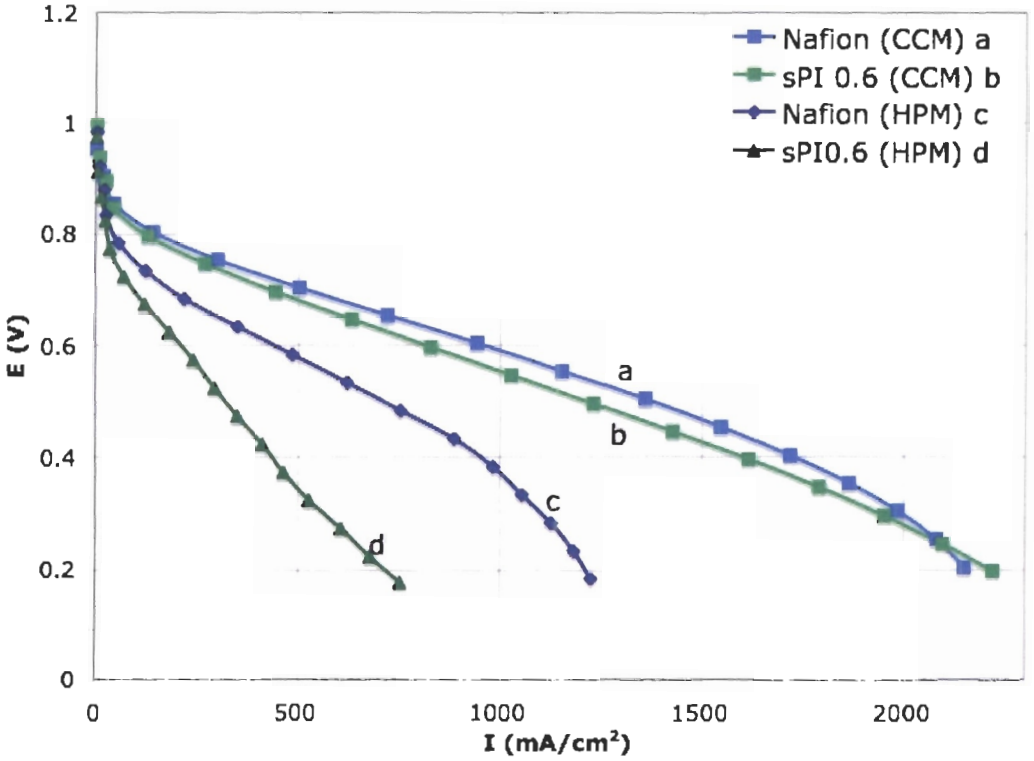

Figure 43: Fuel cell test performance at fully humidified conditions for Nafion® 112 (CCM (a)), Nafion® 115 (HPM (c)) and sPI 0.6 (CCM (b), HPM (d)) at 50°C

CHAPTER 4: CONCLUSION

A series of novel sulfonated polyimides (sPI) containing sulfonated aromatic side chains was synthesized using a novel sulfonated monomer. The successful synthesis of sPI was verified by the ^{1}H NMR spectra, the aromatic/aliphatic proton integral ratio, the ion exchange capacity (from both titration and ^{1}H NMR) and through FTIR.

A series of sulfonated polyimides was evaluated for ion exchange capacity, water uptake, volume uptake, proton conductivity, and hydrolytic stability. The hydrolytic stability was improved in comparison to linear and rigid sulfonated polyimides previously synthesized in-house. This was probably due to a higher basicity of the amine groups in the modified polymer and possibly due to a better phase separation of the hydrophilic and hydrophobic domains. Preliminary studies indicated the polymer membrane shows an encouraging performance in a fuel cell operated at 50°C.

The route used to synthesize sulfonated monomers developed in this work can be used to synthesize other novel sulfonated monomers. Studies of sulfonated polyimides reported in the literature focus on the effect of the non-sulfonated components. It would be interesting to synthesize sulfonated monomers in order to modify the properties of the polymer backbone and to affect the polymer's flexibility and hydrophobicity. Figure 44 shows the possible monomers that could be made using this method as a means for future study.

The fluorinated groups on **21** should increase the backbone hydrophobicity and increase the hydrolytic stability due to a better phase separation. The ether bond in **23** should help increase the hydrolytic stability of the polymer by increasing backbone relaxation. Monomer **21**, **22** and **23** could be used to study the effect of a spacer in the sulfonated monomer on the properties of the resultant polymer.

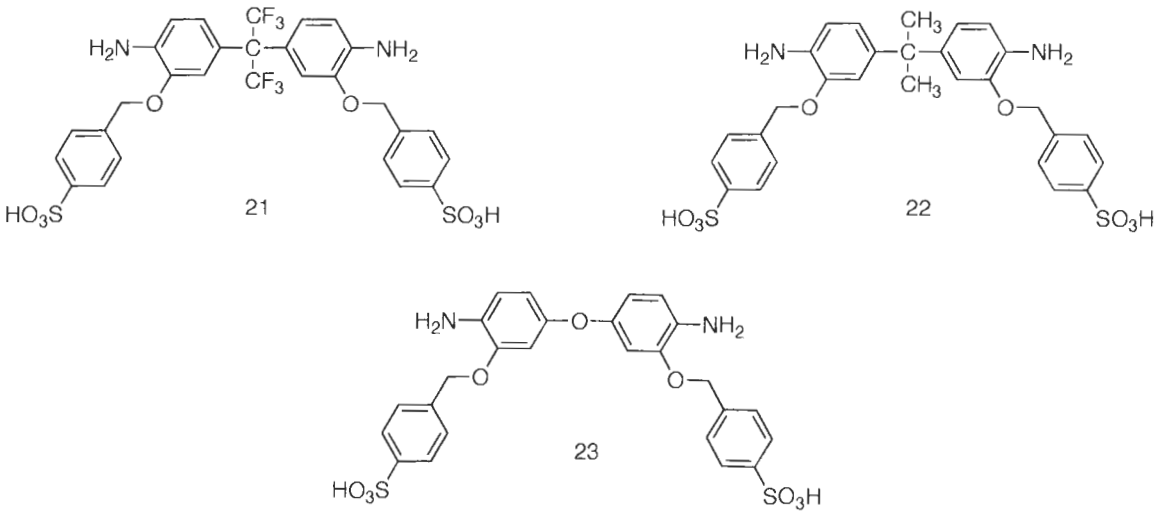

Figure 44: Alternative sulfonated monomers for preparing sulfonated polyimides.

CHAPTER 5: EXPERIMENTAL

This section describe the synthesis and the characterization of the sulfononated monomer (2,2'-bis(4-sulfobenzyloxy)benzidine) and the series of sulfonated polyimides (sPI). The starting materials were bought from Sigma Aldrich and were used as received.

5.1 Synthesis

5.1.1 Synthesis of 4-(bromomethyl)benzene sulfonic acid (1)

See Figure 25 (page 33) for reaction scheme.

1st step[6]: Benzylamine (**4**) (1 mL, 9.155 mmol) was added dropwise to 1 mL of ice-cooled, concentrated sulfuric acid. The mixture was allowed to warm to room temperature before adding 3 mL of 30% oleum. The new mixture was poured into ice-water and the precipitate filtered, washed with water, methanol and finally ether to give 0.8 g of the crude product. Recrystallization from water gave pure **5** (0.60 g, 3.21 mmol) in 35.0% yield.

(**5**) ^{1}H NMR (DMSO-d_6, 500 MHz) δ 7.53 (2H, d), 7.21 (2H, d), 3.69 (2H, s), 2.72 (2H, br)

2nd step: A suspension of **5** (1.1235 g, 6.0016 mmol) in 0.04M solution of sodium acetate was adjusted to pH 3.3 and treated drop wise with sodium nitrite (0.4141 g, 6.002 mmol) at 40°C until it dissolved. The solution was evaporated

and the residue taken up in water and transferred onto a cationic exchanger IRC-50 for 24 hours. After filtration, the solution was evaporated, dissolved in methanol, treated with ether and filtered to give **6** (0.5911 g, 2.812 mmol) for a yield of 46.9%.

(**6**) ^{1}H NMR (DMSO-d_6, 500 MHz) δ 7.51 (2H, d), 7.25 (2H, d), 5.20 (1H, t), 4.49 (2H, d)

3rd step: **6** (4.9610 g, 23.604 mmol) was treated with 65 mL 33% wt.% HBr in acetic acid solution for 48 h at room temperature. The solution was evaporated and the residue taken up in methanol, treated with ether and filtered to give **1** (6.1460 g, 22.424 mmol) for a yield of 95%. **(1)** ^{1}H NMR (DMSO-d_6, 500 MHz) δ 7.59 (2H, d), 7.38 (2H, d), 4.69 (2H, s)

5.1.2 Synthesis of the Sulfonated Monomer*

See Figure 26 (page 35) for reaction's scheme.

This section describes the synthesis of 2,2'-bis(4-sulfobenzyloxy)benzidine used in the synthesis of the sulfonated polyimide.

1st step: To a suspension of 3,3'-dihydroxybenzidine (**7**) (1.000 g, 4.625 mmol) in 30 mL of anhydrous ethanol was added benzophenone imine (**8**) (1.7604 g, 9.713 mmol). The suspension was refluxed overnight. The light brown suspension turned bright yellow after 5 h. The suspension was then filtered and washed with methanol to give the pure bright yellow compound (N,N'-bis(diphenylmethylene)-o-aminophenol (**9**)) with a yield of 88%.

* A similar synthetic route was used by Yasuda et al. in *Journal of Polymer Science Part A-Polymer Chemisty*, 2006, 44(13), 3995-4005.

^{1}H NMR (**9**) (DMSO-d_6, 500 MHz) δ 9.07 (1H, s), 7.64 (2H, d, 7.0 Hz), 7.51 (1H, t), 7.44 (3H, m), 7.29 (2H, t, 8.0 Hz), 7.16 (2H, d, 7.5 Hz), 6.85 (1H, s), 6.68 (1H, d, 8 Hz), 6.37 (1H, d, 8Hz)

^{13}C (**9**) (DMSO-d_6, 100 MHz) δ 168.19, 147.87, 138.97, 138.42, 136.49, 135.44, 130.78, 128.23, 120.69, 116.36, 112.75

FTIR (**9**) (KBr cm^{-1}): 3200(O-H stretch), 3050 (Ar-H stretch), 1588 (C=C stretch), 1560 (C=N stretch), 1480 (C=C stretch), 1323 (C-N stretch), 1188 (C-O stretch)

EA (**9**): Calcd for $C_{38}H_{28}O_2N_2$: C, 83.80; H, 5.18; N, 5.14 Found: C, 83.55; H, 5.39; N, 4.91

2nd step: To a suspension of **9** (1.0000 g, 1.921 mmol) and **1** (1.0129 g, 4.034 mmol) in DMF was added sodium hydride (0.0968 g 4.03 mmol). The reaction was left stirring overnight under nitrogen at room temperature. The yellow suspension turned instantly red after adding NaH and became soluble after 2h, with a red precipitate forming after approximately 5h. Methanol was added to the solution and the white precipitate filtered and washed with methanol to give **10**. The yield was not measured since this product was not purified and characterized.

3rd step: **10** was acidified with 2M HCl for 24 h to remove the protecting groups. The remaining solid was filtered and rinsed with Millipore water. The intermediate was then solubilized in 1M NaOH. The reddish solution was then filtered to remove the insoluble products. The filtrate was then poured in 2M HCl

and gives a light brown precipitate. The precipitate was then isolated by centrifugation and dried under vacuum at 80°C overnight. The dry product was washed with chloroform to give 2,2'-bis(4-sulfobenzyloxy)benzidine (**11**). The total yield for steps 2 and 3 was 83%.

^{1}H NMR **(11)** (DMSO-d_6, 500 MHz) δ 7.61 (2H, d, 8.0 Hz), 7.47 (2H, d, 8.0 Hz), 7.06 (1H, d), 6.89 (1H, dd, 8.5Hz), 6.66 (1H, d, 8Hz), 5.14 (2H, s), 4.68 (2H, s)

^{13}C **(11)** (DMSO-d_6, 100 MHz) δ 152.97, 150.79, 142.99, 141.52, 134.74, 132.03, 130.77, 123.80, 119.57, 115.35, 74.47

FTIR **(11)** (KBr cm^{-1}): 3405 to 2621 (NH_3 stretch), 3050 (Ar-H stretch), 2919 (C-H stretch), 1628 (N-H rocking), 1502 (C=C stretch), 1398 (N-H rocking), 1270 (C-N stretch), 1238 (S=O assym. stretch), 1123 (S=O sym. stretch), 1030 (C-O stretch)

EA **(11)**: Calculated for $C_{26}H_{24}O_8N_2S_2$: C, 56.10; H, 4.35; N, 5.03 Found: C, 55.89; H, 4.54; N, 4.90

5.1.3 Synthesis of Sulfonated Polyimides ($sPI_{0.6}$)

See figure 31 (page 43) for reaction scheme.

To a dry, three necked flask equipped with a Dean Stark trap and condenser was added 2,2'-bis(4-sulfobenzyloxy)benzidine (**11**) (0.2783 g, 0.5000 mmol), 4,4'-oxybisbenzenamine (**13**) (0.06674 g, 0.3333 mmol) and 1,4,5,8-naphthalenetetracarboxylic dianhydride (**14**) (0.2235 g, 0.8333 mmol) under nitrogen. The solvent, m-cresol (5 mL), was added followed by chlorobenzene (7 mL) and triethyl amine (0.1214 g, 1.200 mmol). The mixture was stirred for 2

- 3 hours until complete dissolution of the monomers occurred. Benzoic acid (0.1221 g, 1.000 mmol) was then added to the solution and the temperature increased to 150°C for 2 h. The chlorobenzene was then removed from the solution and the temperature was brought to 180°C for 24h. After cooling down the solution, 10 mL of m-cresol was added to the solution. Finally, the polymer was precipitated in methanol.

After filtration, the remaining m-cresol was removed using a Soxhlet extractor with methanol as solvent for 48h. The polymer was then dried under vacuum at 80°C for 24h and dissolved in DMSO. The viscous solution was then filtered and cast on a flat glass petri dish at 80°C for 24h. Based on the feed ration of monomers, the yield of the reaction is 99%.

A series of six polymers was synthesized by changing the feed ratio of the monomers. The molar ratio of sulfonated monomer (**11**) and non-sulfonated monomer (**13**) was changed to obtain different ion exchange capacity.

^{1}H NMR ($sPI_{0.6}$) (DMSO-d_6, 500 MHz) δ 8.78 (br), 7.77 (br), 7.56 (br), 7.49 (br), 7.39-7.22 (br), 5.28 (br)

FTIR (drop cast on NaCl cm^{-1}): 3442 (H_2O/O-H stretch), 3074-3007 (Ar-H stretch), 2915 (C-H stretch), 1715 (C=O sym. stretch), 1675 (C=O asym. stretch), 1582 (C=C stretch), 1499 (C=C stretch), 1448 (C=C stretch), 1349 (C-N stretch), 1251 (Ar-O stretch), 1199 (C-O stretch), 1123 (S=O stretch), 1037 (SO_3 sym. stretch), 1012 (S-OH stretch)

5.1.4 Membrane Casting

Polymers were precipitated from methanol. Soxhlet extraction with methanol was carried out on the precipitated polymers for 48 h to remove residual m-cresol. It was then dried in a vacuum oven at reduced pressure at 80°C overnight. The dry polymers were dissolved in DMSO. Solutions were filtered and spread on a flat Petri dish. The solvent was evaporated at 80°C until the membrane formed. The membrane was then cut into rectangular pieces (~1 cm x 2 cm) before characterization. Figure 45 shows the process of membrane casting.

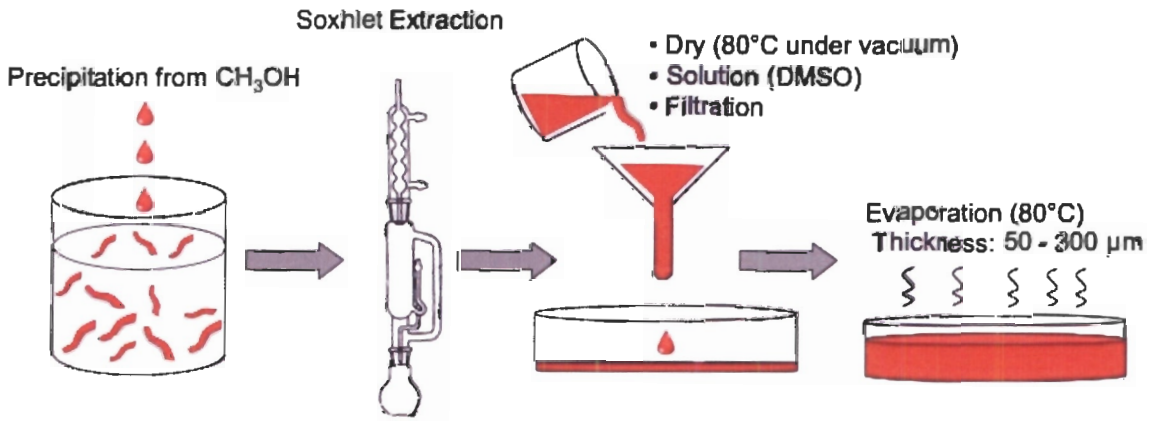

Figure 45: General process of membrane casting of sulfonated polyimides

5.2 Instrumentation

5.2.1 Nuclear magnetic resonance (NMR)

^{1}H NMR spectra were obtained on a Varian Unity Spectrometer 500 MHz operating at 500MHz and ^{13}C NMR spectra from a Bruker Unity Spectrometer 400MHz operating at 100.4 MHz. The compounds were dissolved in DMSO-d_6 at a concentration of ~10 mg/mL. Triethylamine was added to the sulfonated

monomer solution to increase its solubility. For the sulfonated polyimides, the salt form ($SO_3^-(CH_3CH_2)_3NH^+$) was used due to its higher solubility compared to the acid form.

5.2.2 Fourier transform infrared spectroscopy (FTIR)

The instrument used was a Bomem FTLA2000-154 FTIR system. For the sulfonated monomer and its intermediate, KBr pellets were made with the appropriate compound. Sulfonated polyimides (sodium form) were drop-cast from a DMSO solution on a NaCl window and dried under vacuum at 80°C for 2 hours prior to measurements.

5.2.3 Elemental analysis

Elemental analysis was used to determine the composition of the sulfonated monomer (**12**) and its intermediate (**10**). Elemental analysis was performed by Dr. Miki Yang on a Carlo Erba model 1106 CHN analyzer.

5.2.4 Differential scanning calorimetry (DSC)

Measurements were performed on the sulfonated polyimides (acid form) by Marianne Rodgers on a DSC Q10 instrument at a rate of 10°C/min under nitrogen from 30°C to 550°C. Prior to measurement, the samples were dried at 150°C for 30 minutes in the instrument chamber to remove excess water.

5.2.5 Thermogravimetric analysis (TGA)

Measurements were performed on the sulfonated polyimides (acid form) by Marianne Rodgers on a 2950 TGA HR instrument at a rate of 10°C/min under

nitrogen from 50°C to 550°C. Prior to measurement, the samples were dried at 150°C for 30 minutes in the instrument chamber to remove excess water.

5.3 Characterization procedures

5.3.1 Viscosity determination

The measurements of reduced and inherent viscosity of synthesized sulfonated polyimides were performed using a homemade viscometer, thermally controlled by a circulating water system. An automatic timer, controlled by a refractive index detector, was used to make the time measurements. Viscosities were measured at 30°C in m-cresol. Viscosity provides information on the size of a polymer molecule in solution.

The measurements of reduced and inherent viscosity of synthesized sulfonated polyimides were performed using a homemade viscometer, thermally controlled by a circulating water system.

Inherent and reduced viscosity were measured and compared with literature values.[78] Equation 1 and 2 were used to respectively calculate the reduced and inherent viscosity

$$(1) \qquad \eta_{red} = \frac{\eta_{sp}}{[polymer]}$$

$$(2) \qquad \eta_{inh} = \frac{\ln(\eta_r)}{[polymer]}$$

η_{red} and η_{inh} can be calculated using equations 3 and 4. Considering that the viscosities are measured for dilute solution, and knowing that $\eta = A\rho t$ (where A is a constant for a given viscometer and ρ is the density), $\eta_r = t/t_0$ (for dilute solution, $\rho \sim \rho_0$).[78]

$$\eta_{sp} = \eta_r - 1 \qquad (3)$$

$$\eta_r = \frac{\eta}{\eta_0}^{(1)} = \frac{\rho t}{\rho_0 t_0}^{(2)} = \frac{t}{t_0} \qquad (4)$$

(1) η_0 is the viscosity of the solvent and η is the viscosity of a polymer solution at a concentration [polymer] (g/dL). (2) t and t_0 are the flow times of a polymer solution of concentration c and the pure solvent respectively.

The next two equations show a typical calculation of inherent and reduced viscosity for $sPI_{0.6}$ at the highest concentration (0.6075 g/dL). The flow time for the pure solvent (t_0) and the polymer solution (t) are respectively 53.33 s and 13.56 s.

$$\eta_{inh} = \frac{\ln(\eta_r)}{[sPI_{0.6}]} = \frac{\ln(t/t_0)}{[sPI_{0.6}]} = \frac{\ln(53.33s/13.56s)}{0.6075 g dL^{-1}} = 2.255\ dLg^{-1}$$

$$\eta_{red} = \frac{\eta_{sp}}{[sPI_{0.6}]} = \frac{\eta_r - 1}{[sPI_{0.6}]} = \frac{(t/t_0) - 1}{[sPI_{0.6}]} = \frac{(53.33s/13.56s) - 1}{0.6075 g dL^{-1}} = 4.830 dLg^{-1}$$

5.3.2 Water uptake

After casting, the membrane was soaked in 2 M HCl for 48 h. The membrane was then rinsed and soaked for 2 h in Millipore water. The membrane was dried in a vacuum oven at 80°C under reduced pressure for 24 h. The dry membrane was then weighed, soaked again in Millipore water for 48 h, and weighed again.

The water uptake is reported as a percentage uptake and determined by

taking the equilibrium weight difference between the wet film (W_{wet}) and the dry film (W_{dry}) and dividing by the dry film (W_{dry}) weight. The equation is given below.

$$(5) \quad Water\ Uptake = \frac{w_{wet} - w_{dry}}{w_{dry}} \times 100$$

To obtain the value of water uptake of a membrane, the average water uptake of three membranes with the same theoretical ion exchange capacity was measured.

The next equation shows a typical water uptake calculation ($sPI_{0.6}$). The dry (w_{dry}) and wet (w_{wet}) weights were 16.1 mg and 27.1 mg.

$$Water\ Uptake = \frac{w_{wet} - w_{dry}}{w_{dry}} \times 100 = \frac{27.1mg - 16.1mg}{27.1mg} \times 100 = 40.5\,\%$$

5.3.3 Volume uptake

The acidified membranes were first immersed in Millipore water for 24h. Membranes thickness was measured with Mitutoyo Quickmike Series 293 caliper. Length and width were measured with a Mitutoyo Digimatic Calipers (Series 500). The membranes were dried under vacuum at 80°C overnight. Their volume was then re-measured.

The volume uptake was calculated using equation **6**. It is followed by a water uptake calculation example for $sPI_{0.6}$. The dry (V_{dry}) and wet (V_{wet}) volumes were 7.74 mm^3 and 11.72 mm^3.

$$(6) \qquad Volume\ Uptake = \frac{(V_{wet} - V_{dry})}{V_{dry}} \times 100$$

$$Volume\ Uptake = \frac{(V_{wet} - V_{dry})}{V_{dry}} \times 100 = \frac{11.72\ mm^3 - 7.74\ mm^3}{7.74\ mm^3} \times 100 = 51.4\%$$

5.3.4 Ion exchange capacity from titration (IEC_T)

A typical sulfonated polyimide titration is conducted as follows: sodium hydroxide was used as titrant (0.02 N) for the titration of sulfonic acid groups in the polymer. The titrant was standardized against dry potassium biphthalate immediately prior to titrating. Acidified sulfonated polymers were dried overnight at ~80 °C under vacuum before being weighed. The membrane was then immersed in 2N NaCl solution for one hour to obtain the sodium form and release protons. The end-point was detected by using phenolphthalein.

Ion exchange capacity is defined as the millimolar equivalents of reactive $-SO_3H$ sites per gram of polymer and has units, of mmeq/g. The measured ion exchange capacity values are compared to the theoretical or calculated ion exchange capacity value based on the moles of sulfonated monomer charged to the reaction flask.

The end point was used to calculate the ion exchange capacity (meq/g) of the sulfonated membrane. The reported experimentally-determined ion exchange capacities are the average of at least three separate titrated samples. Equation (7) was used to calculate the ion exchange capacity. The volume of NaOH used to reach the end point (V_{NaOH}), the concentration of the NaOH

solution used ([NaOH]) and the dry weight of the membrane ($w_{membrane}$) were needed to calculate the ion exchange capacity.

$$(7) \qquad IEC = \frac{V_{NaOH} \times [NaOH]}{W_{membrane}} \times 1000$$

The next equation shows an ion exchange capacity (IEC_T) calculation example for $sPI_{0.6}$. The volume of NaOH (0.009 mol/L) needed to neutralize the solution was 7.74 x 10^{-3} L. The membrane's dry weight (w_{dry}) was 40.7 x 10^{-3} g.

$$IEC_T = \frac{V_{NaOH} \times [NaOH]}{W_{dry}} \times 1000 = \frac{7.74 \times 10^{-3} L \times 0.009 molL^{-1}}{40.7 \times 10^{-3} g} \times 1000 = 1.71 mmol g^{-1}$$

5.3.5 Ion exchange capacity from H^1 NMR (IEC_{NMR})

^{1}H NMR was used to confirm the polymer structure and to measure the ion exchange capacity (IEC_{NMR}) and compare the results with the titration method (IEC_T). To determine the ion exchange capacity, the ratio between the aliphatic protons (only present in the sulfonated monomer (SM)) and the aromatic protons (present in SM and other monomers (M)) was measured.

This ratio, based on the molar feed ratio ($Ratio_{FR}$), was compared with the ratio obtained from the peak integration in ^{1}H NMR specta ($Ratio_{NMR}$). Equation 8 was used to calculate the aromatic/aliphatic protons ratio from the molar feed ratio. The number of aromatic protons in the sulfonated part ($H(SM_{Aromatic})$), in

the non-sulfonated part ($H(M_{Aromatic})$ and the aliphatic proton ($H(SM_{Aliphatic})$) were needed.

$$(8) \qquad Ratio = \frac{H_{Aromatic}}{H_{Aliphatic}} = \frac{(H(SM_{Aromatic}) \times (x)) + (H(M_{Aromatic}) \times (1-x))}{H(SM_{Aliphatic})}$$

The next equation shows an example of the calculation of the aromatic/aliphatic protons ratio obtained from the molar feed ratio (for $sPI_{0.6}$ where x = 0.6).

$$Ratio = \frac{H_{Aromatic}}{H_{Aliphatic}} = \frac{(H(SM_{Aromatic}) \times (x)) + (H(M_{Aromatic}) \times (1-x))}{H(SM_{Aliphatic})} = \frac{(18 \times 0.6) + (12 \times (1-0.6))}{4 \times 0.6} = 6.50$$

The ion exchange capacity from NMR (IEC_{NMR}) was obtained using Equation 9. The aromatic/aliphatic proton ratio obtained from NMR ($Ratio_{NMR}$) and molar feed ratio were first calculated.

$$(9) \qquad IEC_{NMR} = \frac{IEC_{FR} \times Ratio_{NMR}}{Ratio_{FR}}$$

The next equation shows an ion exchange capacity (IEC_{NMR}) calculation example for $sPI_{0.6}$. The ion exchange capacity obtained by the molar feed ratio (IEC_{FR}) was 1.73 mmol/g. The aromatic/aliphatic protons ratios obtained from feed ($Ratio_{FR}$) and NMR ($Ratio_{NMR}$) were 6.50 and 6.98, respectively.

$$IEC_{NMR} = \frac{IEC_{FR} \times Ratio_{NMR}}{Ratio_{FR}} = \frac{1.73 mmol/g \times 6.98}{6.50} = 1.85 mmol/g$$

5.3.6 Lambda (λ)

This value represents the average number of water molecules for each sulfonated groups. It can be calculated using the value obtained for the water uptake (WU) and ionic exchange capacity obtained by titration (IEC_t) using the Equation 10.[67]

$$(10) \qquad \lambda = \frac{((WU/100)/MW\ H_2O)}{IEC_T \times 1000^{-1}}$$

The next equation shows a calculation example of lambda for $sPI_{0.6}$. The ion exchange capacity (IEC_T) and water uptake (WU) are 1.73 mmol/g and 39.8%, respectively. The water molecular weight used is 18 mol/g.

$$\lambda = \frac{((WU/100)/MW\ H_2O) \times 1000}{IEC} = \frac{((39.8\%/100)/18\ g\,mol^{-1})}{1.73\ mmol\,g^{-1} \times 1000^{-1}} = 13$$

5.3.7 Proton conductivity

The membrane resistivity (R) was measured with a Solartron SI-1260 Impedance/Gain phase analyser at an alternative current of 0.1 mA in a frequency range between 10 MHz and 100 Hz. The environmental conditions of temperature and relative humidity were controlled with an Espec SH-241 Environmental Chamber. Figure 46 illustrates the cell used for conductivity measurements. The length (l) and width (w) were measured with a pair of Mitutoyo Digimatic Calipers Series 500 and the thickness (t) was measured with a Mitutoyo Quickmike Series 293. The membranes resistivity was calculated using Zplot 2.8 for windows (Scribner Associates, Inc.).

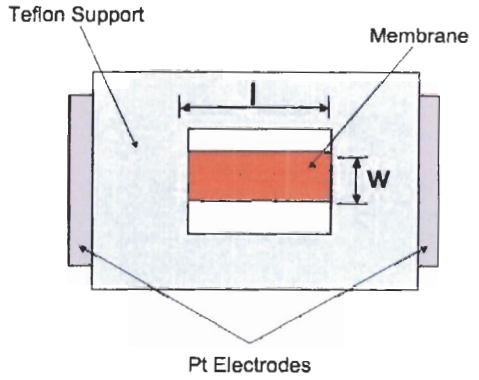

Figure 46: Conductivity cell

The proton conductivity (σ) is calculated using Equation 11. The membranes length (l), width (w) and thickness (t) were measure prior to the resistivity measurement. Membrane resistance (R_M) was measured by impedance spectroscopy and obtained using Zplot 2.8 for Windows (Scribner Associates, Inc.). The system used in this work can be represented as an equivalent circuit (Figure 47) where R_s (solution resistance), C_{dl} (bulk capacitance) and R_M (membrane resistance) are the main components. The relationship between the applied potential and the current flow is known as the impedance, which is analogous to the resistance-current-potential relationship of a dc circuit. The impedance (Z) has a magnitude ($\Delta E/\Delta i$) and phase (f) and is thus a vector quantity. Figure 49 shows a typical result obtained for our system. The important feature is the diameter of the semi-circle. The larger it is, the higher is the resistance. At low frequency (the right side of the semi-circle)where it intersects the Z axis, the system is considered as pure resistance. When the frequency increases, the membrane capacitance influences the impedance. The

combination of the capacitance and resistance leads to the semi-circle. Due, to the complexity of the results, a software (Zplot 2.8) is needed to extract the membrane resistance (R_M). Results obtained at 30°C and 95% relative humidity are presented in Table 8.

$$\sigma = \frac{l}{R_M \times w \times t} \quad (11)$$

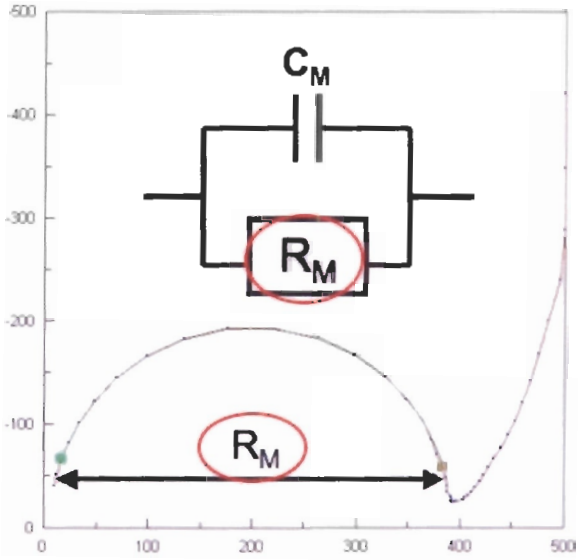

Figure 47: A typical impedance plot from which conductivity data is calculated

The next equation shows an example of a calculation of conductivity (for $sPI_{0.6}$ (σ)) at 30°C and 95 %RH. The length (l), width (w), thickness (t) and membrane resistance (R_M) were 0.50 cm, 0.78 cm, 0.005 cm and 4384 Ohm respectively.

$$\sigma = \frac{l}{R_M \times w \times t} = \frac{0.50\,cm}{4384\,\Omega \times 0.78\,cm \times 0.005\,cm} = 0.027\,S\,cm^{-1}$$

5.3.8 Membrane stability

The hydrolytic stability of the sulfonated polyimide membrane was determined by immersing the membranes into distilled water at 80°C and characterized by the loss of mechanical strength. The mechanical stability test was made every 20 minutes for the first hour, every hour for five hours and once a day until they lost their mechanical property as judged by the bend test. The same test was simultaneously performed on the other membranes. Figure 48 shows the steps followed for the membrane stability tests.

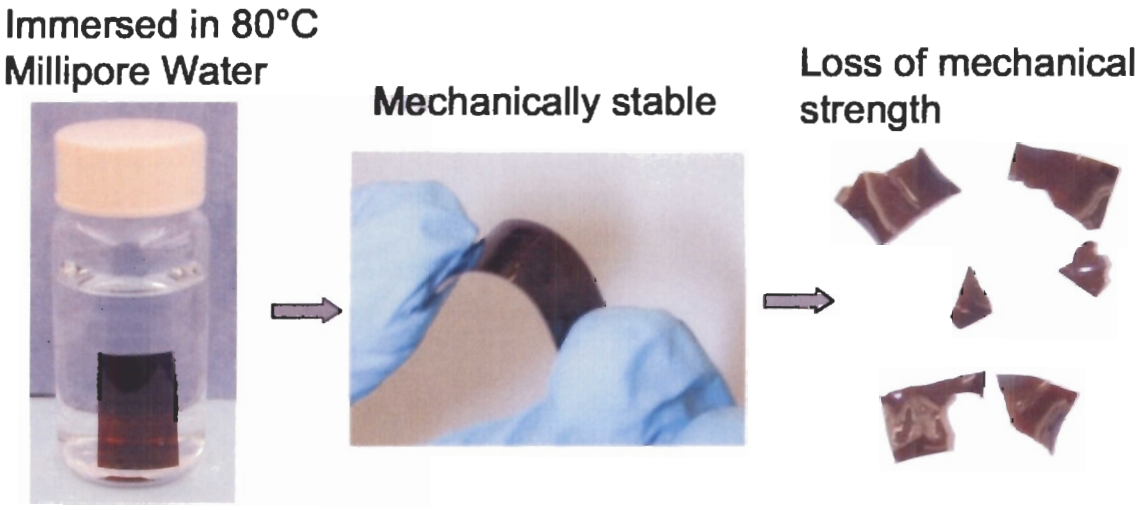

Figure 48: Example of the hydrolytic stability test

5.3.9 Fuel cell test

Two different techniques were used to form the membrane electrode assembly (MEA). Hot pressed membrane (HPM) and catalyst coated membrane (CCM) were assembled before testing.

For the hot pressed membrane method, the sublayer was composed of 0.5 mg/cm^2 Carbon (PEMEAS, E-TEK Division) with 10% PTFE (Sigma-Aldrich Co.).

The catalyst was made of 0.25 mg/cm^2 20% Pt/C (PEMEAS, E-TEK Division) with 30% wt Nafion® (Sigma-Aldrich Co.) ionomer spread on Toray carbon paper 10%, wetproofed (PEMEAS, E-TEK Division).

For the catalyst coated membrane method, SGL's BC24 Gas Diffusion Media (GDM) (SGL Carbon Group) containing a microporous Layer (MPL) deposited were used as the electrodes. An ink slurry was prepared and sprayed directly on the membrane. An ink slurry was prepared to have the composition of 0.4 mg/cm^2 carbon supported (Vulcan XC-72) Pt (PEMEAS, E-TEK Division) and 30 wt% Nafion ionomer content. The catalyst coated membrane was first laminated with a 38 μm laminating pouch as an integration of subgasket. A 125 μm thick compressable Si-gasket was used to assemble the gas diffusion media.

A triple serpentine 5 cm^2 single cell (Teledyne Energy Systems) was used for this experiment. The cell was operated with 200 mL/min of H_2 and O_2 for anode and cathode, respectively. Gases were fully humidified and supplied in a co-flow manner. The cell temperature was set at 50 ºC and each point of the polarization curve was obtained by controlling the potential from open circuit voltage (OCV) to 0.2 V by holding for 60 seconds at 50 mV increments. Fuel cell tests were performed by Makoto Adachi at the National Research Council-IF.

REFERENCES

1. Schoenbein, C. F., On the Voltaic Polarization of certain Solid and fluid substances. *Philosophical Magazine (III)* **1839,** 14, 43.

2. Grove, W. R., On Voltaic Series and the Combination of Gases by Platinum. *Philosophical Magazine* **1839,** 14, 127.

3. Grove, W. R., On a Gaseous Voltaic Battery. *Philosophical Magazine (III)* **1842,** 21, 417.

4. Ostwald, W., *Journal of Electric Energy* **1894,** 1, 122.

5. Larminie, J.; Dicks, D., *Fuel Cell Systems Explained.* Second ed.; John Wiley & Sons Ltd: England, 2003; Vol. 1, p 406.

6. Affanni, A.; Bellini, A.; Franceschini, G.; Guglielmi, P.; Tassoni, C., Battery choice and management for new-generation electric vehicles. *Ieee Transactions on Industrial Electronics* **2005,** 52, (5), 1343-1349.

7. Rikukawa, M.; Sanui, K., Proton-conducting polymer electrolyte membranes based on hydrocarbon polymers. *Progress in Polymer Science* **2000,** 25, (10), 1463-1502.

8. Gottesfeld, S., Foreword. In *Handbook of fuel cells : fundamentals, technology, and applications*, Vielstich, W. L., A.; Gasteiger, H.A., Ed. Wiley: New York, 2004; Vol. 1, p 449.

9. Hickner, M. A.; Ghassemi, H.; Kim, Y. S.; Einsla, B. R.; McGrath, J. E., Alternative polymer systems for proton exchange membranes (PEMs). *Chemical Reviews* **2004,** 104, (10), 4587-4611.

10. Smitha, B.; Sridhar, S.; Khan, A. A., Solid polymer electrolyte membranes for fuel cell applications - a review. *Journal of Membrane Science* **2005,** 259, (1-2), 10-26.

11. Carrette, L.; Friedrich, K. A.; Stimming, U., Fuel cells: Principles, types, fuels, and applications. *Chemphyschem* **2000,** 1, (4), 162-193.

12. Vielstich, W., Ideal and effective efficiencies of cell reactions and comparison to carnot cycles. In *Handbook of fuel cells : fundamentals, technology, and applications*, Vielstich, W. L., A.; Gasteiger, H.A., Ed. Wiley: New York, 2004; Vol. 1, p 449.

13. Mehta, V.; Cooper, J. S., Review and analysis of PEM fuel cell design and manufacturing. *Journal of Power Sources* **2003,** 114, (1), 32-53.

14. Sandstede, G. C., E.J.; Bagotsky, V.S.; Wiesener, K., History of low temperature fuel cells. In *Handbook of fuel cells : fundamentals, technology, and applications*, Vielstich, W. L., A.; Gasteiger, H.A., Ed. Wiley: New York, 2003; Vol. 1, p 449.

15. Zhang, J.; Xie, Z.; Zhang, J.; Tang, Y.; Song, C.; Navessin, T.; Shi, Z.; Song, D.; Wang, H.; Wilkinson, D. P., High temperature PEM fuel cells. *Journal of Power Sources* **2006,** 160, (2), 872-891.

16. Li, Q.; He, R.; Jensen, J. O.; Bjerrum, N. J., Approaches and Recent Development of Polymer Electrolyte Membranes for Fuel Cells Operating above 100 DegC. *Chemistry of Materials* **2003,** 15, (26), 4896-4915.

17. Yin, Y.; Fang, J. H.; Cui, Y. F.; Tanaka, K.; Kita, H.; Okamoto, K., Synthesis, proton conductivity and methanol permeability of a novel sulfonated polyimide from 3-(2 ',4 '-diaminophenoxy)propane sulfonic acid. *Polymer* **2003,** 44, (16), 4509-4518.

18. Kreuer, K. D., On the development of proton conducting polymer membranes for hydrogen and methanol fuel cells. *Journal of Membrane Science* **2001,** 185, (1), 29-39.

19. Yokokawa, H.; Sakai, N., History of hight temperature fuel cell development. In *Handbook of Fuel Cell*, Vielstich, W.; Lamm, A.; Gasteiger, H. A., Eds. John Wiley & Sons Ltd.: Chichester, 2003; Vol. 1: Fundamentals and Survey of Systems, p 449.

20. Hickner, M. A.; Pivovar, B. S., The chemical and structural nature of proton exchange membrane fuel cell properties. *Fuel Cells* **2005,** 5, (2), 213-229.

21. Yang, Y.; Holdcroft, S., Synthetic strategies for controlling the morphology of proton conducting polymer membranes. *Fuel Cells* **2005,** 5, (2), 171-186.

22. Kreuer, K. D.; Paddison, S. J.; Spohr, E.; Schuster, M., Transport in proton conductors for fuel-cell applications: Simulations, elementary reactions, and phenomenology. *Chemical Reviews* **2004,** 104, (10), 4637-4678.

23. Agmon, N., The Grotthuss Mechanism. *Chemical Physics Letters* **1995,** 244, (5-6), 456-462.

24. Mauritz, K. A.; Moore, R. B., State of understanding of Nafion. *Chemical Reviews* **2004,** 104, (10), 4535-4585.

25. M.R. Tant, K. A. M., G.L. Wilkes, *Ionomers: synthesis, structure, properties and applications*. First ed.; Chapman & Hall: New York, 1997; p 514.

26. Adi Eisenberg, J.-S. K., *Introduction to ionomers*. John Wiley & Sons: New York, 1998; p 327.

27. Eæge, S. N.; Kleinman, R.; Carter, M. L. C., *Organic chemistry*. 2nd ed.; D.C. Heath: Lexington, Mass., 1989; p xxv, 1269, 42.

28. Robeson, L. M.; Matzner, M. Flame retardant polyarylate compositions. U.S. Patent 4380598, 1983.

29. Ueda, M.; Toyota, H.; Ouchi, T.; Sugiyama, J. I.; Yonetake, K.; Masuko, T.; Teramoto, T., Synthesis and Characterization of Aromatic Poly(Ether Sulfone)S Containing Pendant Sodium-Sulfonate Groups. *Journal of Polymer Science Part a-Polymer Chemistry* **1993,** 31, (4), 853-858.

30. Wang, F.; Hickner, M.; Kim, Y. S.; Zawodzinski, T. A.; McGrath, J. E., Direct polymerization of sulfonated poly(arylene ether sulfone) random (statistical) copolymers: candidates for new proton exchange membranes. *Journal of Membrane Science* **2002,** 197, (1-2), 231-242.

31. Gieselman, M. B.; Reynolds, J. R., Aramid and imidazole based polyelectrolytes: physical properties and ternary phase behavior with poly(benzobisthiazole) in methanesulfonic acid. *Macromolecules* **1993,** 26, (21), 5633-42.

32. Glipa, X.; El Haddad, M.; Jones, D. J.; Roziere, J., Synthesis and characterization of sulfonated polybenzimidazole: a highly conducting proton exchange polymer. *Solid State Ionics* **1997,** 97, (1-4), 323-331.

33. Karlsson, L. E.; Jannasch, P., Polysulfone ionomers for proton-conducting fuel cell membranes: sulfoalkylated polysulfones. *Journal of Membrane Science* **2004,** 230, (1-2), 61-70.

34. Ohya, H., *Polyimide Membranes*. 1st ed.; Tokyo: Kodansha Ltd.; Amsterdam: Gordon and Breach.: Tokyo and Amsterdam, 1996; Vol. 1, p 314.

35. Ohya, H.; Kudryavtsev, V. V.; Semenova, S. I., *Polyimide membranes : applications, fabrications, and properties*. Kodansha ; Gordon and Breach: Tokyo

Amsterdam, 1996; p x, 314.

36. Bessonov, M. I.; Wright, W. W., *Polyimides--thermally stable polymers*. Consultants Bureau: New York, 1987; p xiv, 318.

37. Cornet, N.; Diat, O.; Gebel, G.; Jousse, F.; Marsacq, D.; Mercier, R.; Pineri, M., Sulfonated polyimide membranes: a new type of ion-conducting membrane for electrochemical applications. *Journal of New Materials for Electrochemical Systems* **2000,** 3, (1), 33-42.

38. Sroog, C. E., Polyimides. *Progress in Polymer Science* **1991,** 16, (4), 561-694.

39. Huang, J. G.; Cranford, R. J.; Matsuura, T.; Roy, C., Sorption and transport behavior of water vapor in dense and asymmetric polyimide membranes. *Journal of Membrane Science* **2004,** 241, (2), 187-196.

40. Yin, Y.; Yamada, O.; Tanaka, K.; Okamoto, K., On the development of naphthalene-based sulfonated polyimide membranes for fuel cell applications. *Polymer Journal* **2006,** 38, (3), 197-219.

41. Rusanov, A. L., Novel Bis(Naphthalic Anhydrides) and Their Polyheteroarylenes with Improved Processability. In *Polymer Synthesis*, 1994; Vol. 111, pp 115-175.

42. Genies, C.; Mercier, R.; Sillion, B.; Petiaud, R.; Cornet, N.; Gebel, G.; Pineri, M., Stability study of sulfonated phthalic and naphthalenic polyimide structures in aqueous medium. *Polymer* **2001,** 42, (12), 5097-5105.

43. Genies, C.; Mercier, R.; Sillion, B.; Cornet, N.; Gebel, G.; Pineri, M., Soluble sulfonated naphthalenic polyimides as materials for proton exchange membranes. *Polymer* **2001,** 42, (2), 359-373.

44. Fang, J.; Guo, X.; Harada, S.; Watari, T.; Tanaka, K.; Kita, H.; Okamoto, K., Novel Sulfonated Polyimides as Polyelectrolytes for Fuel Cell Application. 1. Synthesis, Proton Conductivity, and Water Stability of Polyimides from 4,4'-Diaminodiphenyl Ether-2,2'-disulfonic Acid. *Macromolecules* **2002,** 35, (24), 9022-9028.

45. Cella, J. A., Degradation and Stability of Polyimides. *Polymer Degradation and Stability* **1992,** 36, (2), 99-110.

46. Yin, Y.; Fang, J.; Watari, T.; Tanaka, K.; Kita, H.; Okamoto, K.-I., Synthesis and properties of highly sulfonated proton conducting polyimides from bis(3-sulfopropoxy)benzidine diamines. *Journal of Materials Chemistry* **2004,** 14, (6), 1062-1070.

47. Okamoto, K., Sulfonated polyimides for polymer electrolyte membrane fuel cell. *Journal of Photopolymer Science and Technology* **2003,** 16, (2), 247-254.

48. Yin, Y.; Fang, J.; Kita, H.; Okamoto, K.-I., Novel sulfoalkoxylated polyimide membrane for polymer electrolyte fuel cells. *Chemistry Letters* **2003,** 32, (4), 328-329.

49. Guo, X.; Fang, J.; Watari, T.; Tanaka, K.; Kita, H.; Okamoto, K., Novel Sulfonated Polyimides as Polyelectrolytes for Fuel Cell Application. 2. Synthesis and Proton Conductivity of Polyimides from 9,9-Bis(4-aminophenyl)fluorene-2,7-disulfonic Acid. *Macromolecules* **2002,** 35, (17), 6707-6713.

50. Watari, T.; Fang, J.; Tanaka, K.; Kita, H.; Okamoto, K.-i.; Hirano, T., Synthesis, water stability and proton conductivity of novel sulfonated polyimides from 4,4'-bis(4-aminophenoxy)biphenyl-3,3'-disulfonic acid. *Journal of Membrane Science* **2004,** 230, (1-2), 111-120.

51. Guo, X. X.; Fang, J. H.; Watari, T.; Tanaka, K.; Kita, H.; Okamoto, K. I., Novel sulfonated polyimides as polyelectrolytes for fuel cell application. 2. Synthesis and proton conductivity, of polyimides from 9,9-bis(4-aminophenyl)fluorene-2,7-disulfonic acid. *Macromolecules* **2002,** 35, (17), 6707-6713.

52. Ding, J. F.; Chuy, C.; Holdcroft, S., Enhanced conductivity in morphologically controlled proton exchange membranes: Synthesis of macromonomers by SFRP and their incorporation into graft polymers. *Macromolecules* **2002,** 35, (4), 1348-1355.

53. Yin, Y.; Yamada, O.; Suto, Y.; Mishima, T.; Tanaka, K.; Kita, H.; Okamoto, K., Synthesis and characterization of proton-conducting copolyimides bearing

pendant sulfonic acid groups. *Journal of Polymer Science Part a-Polymer Chemistry* **2005,** 43, (8), 1545-1553.

54. Yin, Y.; Suto, Y.; Sakabe, T.; Chen, S. W.; Hayashi, S.; Mishima, T.; Yamada, O.; Tanaka, K.; Kita, H.; Okamoto, K., Water stability of sulfonated polyimide membranes. *Macromolecules* **2006,** 39, (3), 1189-1198.

55. Asano, N.; Aoki, M.; Suzuki, S.; Miyatake, K.; Uchida, H.; Watanabe, M., Aliphatic/aromatic polyimide lonomers as a proton conductive membrane for fuel cell applications. *Journal of the American Chemical Society* **2006,** 128, (5), 1762-1769.

56. Yin, Y.; Fang, J. H.; Watari, T.; Tanaka, K.; Kita, H.; Okamoto, K., Synthesis and properties of highly sulfonated proton conducting polyimides from bis(3-sulfopropoxy)benzidine diamines. *Journal of Materials Chemistry* **2004,** 14, (6), 1062-1070.

57. Hubbuch, A.; Bindewald, R.; Foehles, J.; Naithani, V. K.; Zahn, H., 4-Sulfobenzyl, a new carboxy protective group. *Angewandte Chemie* **1980,** 92, (5), 394-5.

58. Hvidt, T.; Szarek, W. A.; Maclean, D. B., Synthesis of Enantiomerically Pure Beta-Amino-Alpha-Methylene-Gamma-Butyrolactones by Way of Ozonolysis of Aromatic Alpha-Amino-Acids. *Canadian Journal of Chemistry-Revue Canadienne De Chimie* **1988,** 66, (4), 779-782.

59. Odonnell, M. J.; Boniece, J. M.; Earp, S. E., Synthesis of Amino-Acids by Phase-Transfer Reactions. *Tetrahedron Letters* **1978**, (30), 2641-2644.

60. Groenewoud, W. M., *Characterisation of polymers by thermal analysis*. Elsevier: Amsterdam ; New York, 2001; p 390.

61. Yasuda, T.; Li, Y.; Miyatake, K.; Hirai, M.; Nanasawa, M.; Watanabe, M., Synthesis and properties of polyimides bearing acid groups on long pendant aliphatic chains. *Journal of Polymer Science Part a-Polymer Chemistry* **2006,** 44, (13), 3995-4005.

62. Young, R. J.; Lovell, P. A., *Introduction to Polymers*. 1991.

63. Debye, P., The Intrinsic Viscosity of Polymer Solutions. *Journal of Chemical Physics* **1946,** 14, (10), 636-639.

64. Pals, D. T. F.; Hermans, J. J., New Method for Deriving the Intrinsic Viscosity of Polyelectrolytes. *Journal of Polymer Science* **1950,** 5, (6), 733-734.

65. Zhang, J. L.; Xie, Z.; Zhang, J. J.; Tanga, Y. H.; Song, C. J.; Navessin, T.; Shi, Z. Q.; Song, D. T.; Wang, H. J.; Wilkinson, D. P.; Liu, Z. S.; Holdcroft, S., High temperature PEM fuel cells. *Journal of Power Sources* **2006,** 160, (2), 872-891.

66. Miyatake, K.; Zhou, H.; Watanabe, M., Proton conductive polyimide electrolytes containing fluorenyl groups: Synthesis, properties, and branching effect. *Macromolecules* **2004,** 37, (13), 4956-4960.

67. Detallante, V.; Langevin, D.; Chappey, C.; Metayer, M.; Mercier, R.; Pineri, M., Water vapor sorption in naphthalenic sulfonated polyimide membranes. *Journal of Membrane Science* **2001,** 190, (2), 227-241.

68. Essafi, W.; Gebel, G.; Mercier, R., Sulfonated polyimide ionomers: A structural study. *Macromolecules* **2004,** 37, (4), 1431-1440.

69. Piroux, F.; Espuche, E.; Mercier, R.; Pineri, M., Water vapour transport mechanism in naphthalenic sulfonated polyimides. *Journal of Membrane Science* **2003,** 223, (1-2), 127-139.

70. Rodgers, M.; Yang, Y. S.; Holdcroft, S., A study of linear versus angled rigid rod polymers for proton conducting membranes using sulfonated polyimides. *European Polymer Journal* **2006,** 42, (5), 1075-1085.

71. Wu, H. L.; Ma, C. C. M.; Li, C. H.; Chen, C. Y., Swelling behavior and solubility parameter of sulfonated poly(ether ether ketone). *Journal of Polymer Science Part B-Polymer Physics* **2006,** 44, (21), 3128-3134.

72. Blachot, J. F.; Diat, O.; Putaux, J. L.; Rollet, A. L.; Rubatat, L.; Vallois, C.; Muller, M.; Gebel, G., Anisotropy of structure and transport properties in sulfonated polyimide membranes. *Journal of Membrane Science* **2003,** 214, (1), 31-42.

73. Wu, H. L.; Ma, C. C. M.; Li, C. H.; Lee, T. M.; Chen, C. Y.; Chiang, C. L.; Wu, C., Sulfonated poly(ether ether ketone)/poly(amide imide) polymer blends for proton conducting membrane. *Journal of Membrane Science* **2006,** 280, (1-2), 501-508.

74. Mecheri, B.; D'Epifanio, A.; Di Vona, M. L.; Traversa, E.; Licoccia, S.; Miyayama, M., Sulfonated polyether ether ketone-based composite membranes doped with a tungsten-based inorganic proton conductor for fuel cell applications. *Journal of the Electrochemical Society* **2006,** 153, (3), A463-A467.

75. Ding, J. F.; Chuy, C.; Holdcroft, S., A self-organized network of nanochannels enhances ion conductivity through polymer films. *Chemistry of Materials* **2001,** 13, (7), 2231

76. Weber, A.; Darling, R.; Meyers, J.; Newman, J., Mass transfer at two-phase and three-phase interfaces. In *Handbook of fuel cells : fundamentals, technology, and applications*, Vielstich, W. L., A.; Gasteiger, H.A., Ed. Wiley: New York, 2003; Vol. 1, p 449.

77. Vielstich, W.; Lamm, A.; Gasteiger, H. A., *Handbook of fuel cells : fundamentals, technology, and applications*. Wiley: Chichester, England ; New York, 2003; p 449.

78. Young, R. J.; Lovell, P., *Introduction to polymers*. 2nd ed.; Chapman and Hall: London ; New York, 1991; p x, 443.